The atmospheric impacts of monoterpene ozonolysis on global stabilised Criegee intermediate budgets and SO_2 oxidation: experiment, theory and modelling

Mike J. Newland[1,3], Andrew R. Rickard[2,3], Tomás Sherwen[3], Mathew J. Evans[2,3], Luc Vereecken[4,5], Amalia Muñoz[6], Milagros Ródenas[6], William J. Bloss[1]

[1]{University of Birmingham, School of Geography, Earth and Environmental Sciences, Birmingham, UK}

[2]{National Centre for Atmospheric Science (NCAS), University of York, York, UK}

[3]{Wolfson Atmospheric Chemistry Laboratories, Department of Chemistry, University of York, York, UK}

[4]{Max Planck Institute for Chemistry, Atmospheric Sciences, Hahn-Meitner-Weg 1, Mainz, Germany}

[5]{Institute for Energy and Climate Research, Forschungszentrum Jülich GmbH, Jülich, Germany}

[6]{Fundación CEAM, EUPHORE Laboratories, Avda/Charles R. Darwin 14. Parque Tecnologico, Valencia, Spain}

Correspondence to: M. J. Newland (mike.newland@york.ac.uk)

A. R. Rickard (andrew.rickard@york.ac.uk)

Abstract

The gas-phase reaction of alkenes with ozone is known to produce stabilised Criegee intermediates (SCIs). These biradical/zwitterionic species have the potential to act as atmospheric oxidants for trace pollutants such as SO_2, enhancing the formation of sulfate aerosol with impacts on air quality and health, radiative transfer and climate. However, the importance of this chemistry is uncertain as a consequence of limited understanding of the abundance and atmospheric fate of SCIs. In this work we apply experimental, theoretical and numerical modelling methods to quantify the atmospheric impacts, abundance, and fate, of

the structurally diverse SCIs derived from the ozonolysis of monoterpenes, the second most abundant group of unsaturated hydrocarbons in the atmosphere. We have investigated the removal of SO_2 by SCI formed from the ozonolysis of three atmospherically important monoterpenes (α-pinene, β-pinene and limonene) in the presence of varying amounts of water vapour in large-scale simulation chamber experiments, representative of boundary layer conditions. The SO_2 removal displays a clear dependence on water vapour concentration, but this dependence is not linear across the range of [H_2O] explored. At low [H_2O] a strong dependence of SO_2 removal on [H_2O] is observed, while at higher [H_2O] this dependence becomes much weaker. This is interpreted as being caused by the production of a variety of structurally (and hence chemically) different SCI in each of the systems studied, each displaying different rates of reaction with water and of unimolecular rearrangement/decomposition. The determined rate constants, k(SCI+H_2O), for those SCI that react primarily with H_2O range from $4 – 310 \times 10^{-15}$ cm^3 s^{-1}. For those SCI that predominantly react unimolecularly, determined rates range from $130 – 240$ s^{-1}. These values are in line with previous results for the (analogous) stereo-specific SCI system of *syn*/*anti*-CH_3CHOO. The experimental results are interpreted through theoretical studies of the SCI unimolecular reactions and bimolecular reactions with H_2O, characterised for α-pinene and β-pinene at the M06-2X/aug-cc-pVTZ level of theory. The theoretically derived rates agree with the experimental results within the uncertainties. A global modelling study, applying the experimental results within the GEOS-Chem chemical transport model, suggests that > 97 % of the total monoterpene derived global SCI burden is comprised of SCI whose structure determines that they react slowly with water, and whose atmospheric fate is dominated by unimolecular reactions. Seasonally averaged boundary layer concentrations of monoterpene-derived SCI reach up to 1.4×10^4 cm^{-3} in regions of elevated monoterpene emissions in the tropics. Reactions of monoterpene derived SCI with SO_2 account for < 1 % globally but may account for up to 60 % of the gas-phase SO_2 removal over areas of tropical forests, with significant localised impacts on the formation of sulfate aerosol, and hence the lifetime and distribution of SO_2.

1 Introduction

Chemical oxidation processes in the atmosphere exert a major influence on atmospheric composition, leading to the removal of primary emitted species, and the formation of

secondary products. In many cases either the emitted species or their oxidation products negatively impact air quality and climate (e.g. ozone, which is also a potent greenhouse gas). These reactions can also transform gas-phase species to the condensed phase, forming secondary aerosol that again can be harmful to health and can both directly and indirectly influence radiative transfer and hence climate (e.g. SO_2 oxidation leading to the formation of sulfate aerosol).

Tropospheric gas-phase oxidants include the OH radical, ozone, the NO_3 radical, and halogen atoms. Stabilised Criegee intermediates (SCIs), or carbonyl oxides, have been identified as another potentially important oxidant in the troposphere (*e.g.* Cox and Penkett, 1971; Mauldin et al., 2012). SCIs are thought to be formed in the atmosphere predominantly from the reaction of ozone with unsaturated hydrocarbons, though other processes may be important under certain conditions, e.g. alkyl iodide photolysis (Gravestock et al., 2010), dissociation of the DMSO peroxy radical (Asatryan and Bozzelli, 2008). Laboratory experiments and theoretical calculations have shown SCI to oxidise SO_2 (*e.g.* Cox and Penkett, 1971; Welz et al., 2012; Taatjes et al., 2013), organic (Welz et al., 2014) and inorganic (Foreman et al., 2016) acids (Vereecken et al., 2017), and a number of other important trace gases found in the atmosphere, as well as forming adducts with NO_2 (Taatjes et al., 2014; Vereecken et al., 2017; Caravan et al., 2017). Measurements in a boreal forest (Mauldin et al., 2012) and at a coastal site (Berresheim et al., 2014) have both identified a 'missing' process (in addition to reaction with OH) oxidising SO_2 to H_2SO_4, potentially arising from SCI reactions.

Here, we present results from a series of experimental studies into SCI formation and reactions, carried out under atmospheric boundary layer conditions in the European Photochemical Reactor facility (EUPHORE), Valencia, Spain. We examine the ozonolysis of three monoterpenes with very different structures (and hence reactivities with OH and ozone): α-pinene (with an endocyclic double bond), β-pinene (with an exocyclic double bond) and limonene (with both an endo and exo cyclic double bond). We observe the removal of SO_2 in the presence of each alkene-ozone system as a function of water vapour concentration. This allows us to derive relative SCI kinetics for reaction with H_2O, SO_2, and unimolecular decomposition. Further, we calculate absolute unimolecular rates and bimolecular reaction rates with H_2O for all α-pinene and β-pinene derived SCI at the M06-2X/aug-cc-pVTZ level of theory. A global modelling study, using the GEOS-Chem global chemical transport model,

is performed to assess global and regional impacts of the chemical kinetics of monoterpene SCI determined in this study.

1.1 Stabilised Criegee Intermediate Kinetics

Ozonolysis of an unsaturated hydrocarbon produces a primary ozonide that rapidly decomposes to yield pairs of Criegee intermediates (CIs) and carbonyls (Johnson and Marston 2008). The population of CIs are formed with a broad internal energy distribution giving both chemically activated and stabilised forms. Chemically activated CIs may undergo collisional stabilisation to an SCI, unimolecular decomposition or isomerisation. SCIs can have sufficiently long lifetimes to undergo bimolecular reactions (Scheme 1).

The predominant atmospheric fate for the simplest SCI, CH_2OO, is reaction with water vapour (likely with the dimer ($(H_2O)_2$) (e.g. Berndt et al., 2014; Newland et al., 2015a; Chao et al., 2015; Lewis et al., 2015; Lin et al., 2016a). For larger SCI, both experimental (Taatjes et al., 2013; Sheps et al., 2014; Newland et al., 2015a; Huang et al., 2015) and theoretical (Kuwata et al., 2010; Anglada et al., 2011; Anglada and Sole, 2016, Vereecken et al., 2017) studies have shown that their kinetics, in particular reaction with water, are highly structure dependent. The significant double bond character exhibited in the zwitterionic configurations of mono-substituted SCI leads to two distinct chemical forms: *syn*-SCI (*i.e.* those where an alkyl-substituent group is on the same side as the terminal oxygen of the carbonyl oxide moiety)), and *anti*-SCI (*i.e.* with the terminal oxygen of the carbonyl oxide moiety on the same side as a hydrogen group). The two conformers of CH_3CHOO, which are both mono-substituted, display these properties. This difference in conformer reactivities has been predicted theoretically (Ryzhkov and Ariya, 2004, Kuwata et al., 2010; Anglada et al., 2011; Lin et al., 2016a) and was subsequently confirmed experimentally (Taatjes et al., 2013; Sheps et al., 2014) for the two CH_3CHOO conformers. The significantly faster reaction of *anti*-CH_3CHOO with water is driven by the higher potential energy of this isomer, while more stable SCI, with a methyl group in *syn*-position, such as *syn*-CH_3CHOO or $(CH_3)_2COO$, react orders of magnitude more slowly with water.

To date, the effects of the water dimer, $(H_2O)_2$ on SCI removal have only been determined experimentally for CH_2OO (Berndt et al., 2014; Chao et al., 2015; Lewis et al., 2015;

Newland et al., 2015a; Sheps et al., 2017; Liu et al., 2017) and *anti*-CH_3CHOO (Lin et al., 2016b). Theoretical calculations (Vereecken et al., 2017) have predicted the ratio of the SCI + $(H_2O)_2$: SCI + H_2O rate constants, k_5/k_3, of larger, and more substituted SCI, to be of a similar order of magnitude as for CH_2OO (i.e. 1.5–2.5 × 10^3).

SCI can also undergo unimolecular isomerisation/decomposition in competition with bimolecular reactions. This is likely to be a significant atmospheric sink for *syn*-SCI because of their slow reaction with water vapour (e.g. Huang et al., 2015). Unimolecular reactions of *syn*-CI/SCI are dominated by a 1,4-H-shift, forming a vinyl hydroperoxide (VHP) intermediate (Niki et al., 1987; Rickard et al., 1999; Martinez and Herron, 1987; Johnson and Marston, 2008; Kidwell et al., 2016). Decomposition of the VHP formed in this process is an important non-photolytic source of OH, HO_2, and RO_2 in the atmosphere (Niki et al., 1987; Alam et al., 2013; Kidwell et al., 2016), which can also lead to secondary organic aerosol formation (Ehn et al., 2014). Unimolecular reactions of the *anti*-CI/SCI are thought to be dominated by a 1,3-ring closure, the "acid/ester channel", in which the CI/SCI decomposes, through a rearrangement to a dioxirane intermediate, producing a range of daughter products and contributing to the observed overall HO_x radical yield (Kroll et al., 2002; Johnson and Marston, 2008; Alam et al., 2013).

$$\text{Alkene} + O_3 \xrightarrow{k_1} \phi\text{SCI} + (1-\phi)\text{CI} + \text{RCHO} \quad \text{(R1)}$$

$$\text{SCI} + SO_2 \xrightarrow{k_2} SO_3 + \text{RCHO} \quad \text{(R2)}$$

$$\text{SCI} + H_2O \xrightarrow{k_3} Products \quad \text{(R3)}$$

$$\text{SCI} \xrightarrow{k_d} Products \quad \text{(R4)}$$

$$\text{SCI} + \text{acid} \xrightarrow{k_5} Products \quad \text{(R5)}$$

$$\text{SCI} + (H_2O)_2 \xrightarrow{k_6} Products \quad \text{(R6)}$$

Decomposition of the simplest SCI, CH_2OO, is slow (< 10 s^{-1}) and is not likely to be an important sink in the troposphere (e.g. Newland et al., 2015a; Chhantyal-Pun et al., 2015). This decomposition occurs primarily via rearrangement through a 'hot' acid species, which represents the lowest accessible decomposition channel (Gutbrod et al., 1996; Alam et al., 2011; Chen et al., 2016). However, recently determined unimolecular reaction rates of larger *syn*-SCI are considerably faster. Newland et al. (2015a) reported unimolecular reaction rate

constants for *syn*-CH_3CHOO of 348 (± 332) s^{-1} and for $(CH_3)_2COO$ of 819 (± 190) s^{-1} (assuming k(*syn*-$CH_3CHOO+SO_2$) = 2.9 × 10^{-11} cm^3 s^{-1} (Sheps et al., 2014) and k($(CH_3)_2COO+SO_2$) = 1.3 × 10^{-10} cm^3 s^{-1} (Huang et al., 2015), respectively). Smith et al. (2016) measured the unimolecular decomposition rate of $(CH_3)_2COO$ to be 269 (± 82) s^{-1} at 283 K increasing to 916 (± 56) s^{-1} at 323 K, suggesting the rate to be fast and highly temperature dependent. Novelli et al. (2014), estimated a significantly slower decomposition rate for s*yn*-CH_3CHOO of 20 (3-30) s^{-1} from direct observations of OH formation, while Fenske et al. (2000), estimated the decomposition rate of CH_3CHOO (i.e. a mix of *syn* and *anti* conformers) produced from ozonolysis of *trans*-but-2-ene to be 76 s^{-1} (accurate to within a factor of three).

1.2 Monoterpene Ozonolysis

Monoterpenes are volatile organic compounds (VOCs) with the general formula $C_{10}H_{16}$, which are emitted by a wide range of vegetation, particularly from boreal forests. Total global monoterpene emissions are estimated to be 95 (± 3) Tg yr^{-1} (Sindelarova et al., 2014) - roughly 13 % of total non-methane biogenic VOC emissions. Monoterpene emissions are dominated by α-pinene, which accounts for roughly 34 % of the total global emissions, while β-pinene and limonene account for 17 % and 9 % respectively (Sindelarova et al., 2014). Monoterpenes (mainly α-pinene and limonene) are also present in indoor environments, in significant amounts where cleaning products and air fresheners are in routine use (on the order of 100s of ppbv) (e.g. Singer et al., (2006); Sarwar and Corsi, (2007)), where their ozonolysis products can affect indoor chemistry and health (*e.g.* Rossignol et al., (2013); Shallcross et al., (2014)).

Monoterpenes are highly reactive due to the presence of (often multiple) double bonds. The oxidation of monoterpenes yields a wide range of multi-functional gas-phase and aerosol products. This process can be initiated by OH and NO_3 radicals or by O_3, with ozonolysis having been shown to be particularly efficient at generating low volatility products that can form SOA, even in the absence of sulfuric acid (e.g. Ehn et al., 2014; Kirkby et al., 2016). These highly oxygenated secondary products have received considerable attention in recent years because of their role in affecting the climate through absorption and scattering of solar radiation (the direct aerosol effect). They can also increase cloud condensation nuclei concentrations, which can change cloud properties and lifetimes (the indirect aerosol effect).

They have also been shown to have a wide range of deleterious effects on human health (e.g. Pöschl and Shiraiwa, 2015).

The ozonolysis reaction for monoterpenes is expected to follow a similar initial process to that of smaller alkenes, with cyclo-addition at a double bond giving a primary ozonide (POZ), followed by rapid decomposition of the POZ to yield a CI and a carbonyl (Scheme 1). Stabilisation of the large POZs formed in monoterpene ozonolysis is expected to be negligible (Nguyen et al., 2009). However, a major difference in ozonolysis at endocyclic bonds is that, on decomposition of the POZ, the carbonyl oxide and carbonyl moieties are tethered as part of the same molecule, providing the potential for further interaction of the two. These can react together to form secondary ozonides (SOZ), which may be stable for several hours (Beck et al., 2011). However, while this has been shown to be potentially the major fate in the atmosphere for SCI derived from sesquiterpenes ($C_{15}H_{24}$) (e.g. Nguyen et al., 2009b; Beck et al., 2011; Yao et al., 2014), formation of SOZ is predicted to be small for monoterpene derived SCI because of the high ring strain caused by the tight cyclisation (e.g. Nguyen et al., 2009b). Chuong et al. (2004) predicted formation of a SOZ to become the dominant atmospheric fate for SCI formed in the ozonolysis of endo-cyclic alkenes with a carbon number between 8 and 15, while Vereecken and Francisco (2012) suggested that internal SOZ formation is likely to be limited to product rings containing six or more carbons due to ring strain.

No studies have yet directly determined the reaction rates of the large SCI produced from monoterpene ozonolysis with SO_2 (or any other trace gases). This is owing to the complexities of synthesizing and measuring large SCI. However, Ahrens et al. (2014) concluded that the reaction of the C9-SCI formed in β-pinene ozonolysis with SO_2 is as fast as that determined by Welz et al. (2012) and Taatjes et al. (2013) for CH_2OO and CH_3CHOO respectively (ca. 4×10^{-11} cm^3 s^{-1}) by fitting to the decay of SO_2 in the presence of the ozonolysis reaction. Mauldin et al. (2012) calculated significantly slower reaction rates for an additional oxidant (assumed to be SCI) derived from α-pinene and limonene ozonolysis, with $k(SCI+SO_2)$ determined to be 6×10^{-13} cm^3 s^{-1} and 8×10^{-13} cm^3 s^{-1} for α-pinene and limonene derived SCI respectively. However, it seems likely that the rates calculated by Mauldin et al. (2012) may be substantially underestimated due to the assumption of a very long SCI lifetime (0.2 s) in experiments that were performed at 50 % RH. The calculated rates scale linearly with SCI lifetime and based on reaction rates of smaller SCI with H_2O (reported since the

Mauldin et al. work, e.g. Taatjes et al., 2013) it seems likely that the lifetime of the SCI in their experiments would have been more like $0.1 - 2 \times 10^{-2}$ s, increasing the calculated rate constants by more than an order of magnitude, bringing them into much closer agreement with the rates reported by Ahrens et al. (2014).

Unimolecular reactions of the monoterpene SCI are expected to proceed rapidly through the VHP route if a hydrogen is available for a 1,4 H-shift. Those SCI that cannot undergo this rearrangement may undergo unimolecular reactions via the formation of the dioxirane intermediate, but this is expected to be a much slower process (Nguyen et al., 2009). In contrast to smaller SCI, it has been observed experimentally, and predicted theoretically, that the VHP route will mainly lead to rearrangement to an acid (also yielding an OH radical) rather than decomposition of the molecule (e.g. Ma et al., 2008, Ma and Marston, 2008). As for the smaller alkenes, monoterpene ozonolysis has been shown to be a source of HO_x (e.g. Paulson et al., 1997; Alam et al., 2013), predominantly via the VHP rearrangement. The MCMv3.3.1 (Jenkin et al., 2015) applies OH yields of 0.80, 0.35 and 0.87 for α-pinene, β-pinene and limonene respectively.

1.2.1 α-pinene derived SCI

Decomposition of the α-pinene POZ yields four different C_{10} Criegee intermediates (Scheme 2: CI-1a, 1b, 2a, 2b), with the carbonyl oxide moiety at one end and a carbonyl group at the other. Here, CI-1 is a mono-substituted CI for which both *syn* (1a) and *anti* (1b) conformers exist, while the other, CI-2, is di-substituted, for which two *syn*-conformers (2a and 2b) exist. Ma et al. (2008) infer a relative yield of 50 % for the two basic CI formed, based on the observation that norpinonic acid yields from the ozonolysis of α-pinene and an enone, which upon ozonolysis yields CI-1, are almost indistinguishable.

The total SCI yield from α-pinene was determined to be 0.15 (± 0.07) by Sipilä et al. (2014) in indirect experiments measuring the production of H_2SO_4 from SO_2 oxidation in the α-pinene ozonolysis system. Drozd and Donahue (2011) also determined a total SCI yield of about 0.15 at 740 Torr, from measuring the loss of hydrofluoroacetone in ozonolysis experiments in a high pressure flow system. The MCMv3.3.1 (Jenkin et al., 1997; Saunders et al., 2003; Jenkin et al., 2015) applies a value of 0.20 based on stabilisation of only the mono-substituted CI-1.

1.2.2 β-pinene derived SCI

β-pinene ozonolysis yields two distinct conformers of the nopinone C9-CI (Scheme 3: CI-3 and CI-4), which differ in orientation of the carbonyl oxide group, and CH_2OO. CI-3 and CI-4 are formed in roughly equal proportions with very little inter-conversion between the two (Nguyen et al., 2009). The difference in the chemical behaviour of CI-3 and CI-4, which were often not distinguished in earlier studies, arises from the inability of the carbon attached to the four-membered ring to undergo the 1,4-H-shift that allows unimolecular decomposition via the VHP channel. This was noted in Rickard et al. (1999) as being a reason for the considerably lower OH yield (obtained via the VHP route) from β-pinene ozonolysis compared to that of α-pinene. This difference leads to contrasting unimolecular decomposition rates for the two CI, with Nguyen et al. (2009) predicting a loss rate of *ca.* 50 s^{-1} for CI-3 (via a VHP) and *ca.* 1 s^{-1} for CI-4 (via ring closure to a dioxirane). This result is qualitatively consistent with the experimental work of Ahrens et al. (2014), who determine a ratio of 85:15 for the abundance of SCI-4:SCI-3 about 10 s after the initiation of the ozonolysis reaction, as a consequence of the much faster decomposition rate of SCI-3. Thus the potential for bimolecular reactions to compete with decomposition of SCI-3 and SCI-4 in the atmosphere is very different.

Nguyen et al. (2009) theoretically calculate a total SCI yield from β-pinene ozonolysis of 42 %, consisting of 16.2 % SCI-3, 20.6 % SCI-4, and 5.1 % CH_2OO. Ahrens et al. (2014) assume an equal yield of CI-3 and CI-4 (45 %) with a 10 % yield of CH_2OO; 40 % of the total C9-CI are calculated to be stabilised at 1 atm. If all of the CH_2OO is assumed to be formed stabilised (e.g. Nguyen et al., 2009) then this gives a total SCI yield of 46 %. Earlier experimental studies have tended to determine lower total SCI yields with Hasson et al. (2001) reporting a total SCI yield of 0.27 from measured product yields (almost entirely nopinone) and Hatakeyama et al. (1984) reporting a total SCI yield of 0.25. Winterhalter et al. (2000) determined a yield of 0.16 (± 0.04) for excited CH_2OO from β-pinene ozonolysis, obtained via the nopinone yield and 0.35 for the stabilised C9-CI, giving a total SCI yield of 0.51 of all the CH_2OO is assumed to be stabilised. Also, experimental studies have tended to report higher CH_2OO yields (determined from measured nopinone yields) than theoretical studies. Nguyen et al. (2009) note that this could be because nopinone can also be formed in bimolecular reactions of SCI-4, hence experimental studies may overestimate CH_2OO production. The MCMv3.3.1 incorporates a total SCI yield of 0.25 from β-pinene ozonolysis, with a yield of stabilised C9-CI of 0.102 and a CH_2OO yield of 0.148.

1.2.3 Limonene derived SCI

Limonene has two double bonds at which ozone can react. Theory suggests that reaction at the endocyclic bond is more likely; Baptista et al. (2011) calculate reaction at the endo-cyclic bond to be 84 – 94 % (dependent on the level of theory applied). Zhang et al. (2006) suggest the reaction at the endo-cyclic double bond to be roughly 25 times faster than at the exo-cyclic bond, i.e. leading to a branching ratio of ca. 96 % reaction at the endo bond and the current IUPAC recommendation (IUPAC, 2013) suggests about 95 % of the primary ozone reaction to be at the endo bond. Leungsakul et al. (2005) reported a best fit to measurements from chamber experiments by assuming an 85 % reaction at the endo-cyclic bond and 15 % at the exo-cyclic bond.

Ozone reaction at the endo-cyclic bond of limonene produces four different C_{10} CI (Scheme 4: CI-5a, 5b, 6a, 6b). Similar to CI-1 and CI-2 from α-pinene, CI-5 is a mono-substituted CI for which both *syn* (5a) and *anti* (5b) conformers exist, while the other, CI-6, is di-substituted, for which two *syn*-conformers (6a and 6b) exist. Leungsakul et al. (2005) determined a total SCI yield from limonene ozonolysis of 0.34, consisting of CH_2OO (0.05), CI-7 (0.04), CI-5 (0.15) and CI-6 (0.11). Sipilä et al. (2014) determined a total SCI yield of 0.27 (± 0.12) from indirect experiments measuring the production of H_2SO_4 from SO_2 oxidation in the presence of the limonene-ozone system. The MCMv3.3.1 describes only reaction with ozone at the endocyclic double bond and recommends a total SCI yield of 0.135 with stabilisation of only the mono-substituted CI-5.

2 Experimental

2.1 Experimental Approach

The EUPHORE facility is a 200 m^3 simulation chamber used primarily for studying reaction mechanisms under atmospheric boundary layer conditions. Further details of the chamber setup and instrumentation are available elsewhere (Becker, 1996; Alam et al., 2011), and a detailed account of the experimental procedure, summarised below, is given in Newland et al (2015a).

Experiments comprised time-resolved measurement of the removal of SO_2 in the presence of the monoterpene-ozone system, as a function of humidity. SO_2 and O_3 abundance were

measured using conventional fluorescence (reported precision ± 1.0 ppbv) and UV absorption monitors (reported precision ± 4.5 ppbv), respectively; alkene abundance was determined via FTIR spectroscopy. Experiments were performed in the dark (*i.e.* with the chamber housing closed; $j(NO_2) \leq 10^{-6}$ s^{-1}), at atmospheric pressure (*ca.* 1000 mbar) and temperatures between 287 and 302 K. The chamber is fitted with large horizontal and vertical fans to ensure rapid mixing (*ca*. 2 minutes). Chamber dilution was monitored via the first order decay of an aliquot of SF_6, added prior to each experiment. Cyclohexane (*ca.* 75 ppmv) was added at the beginning of each experiment to act as an OH scavenger, such that SO_2 reaction with OH was calculated to be ≤ 1 % of the total chemical SO_2 removal in all experiments.

Experimental procedure, starting with the chamber filled with clean scrubbed air, comprised addition of SF_6 and cyclohexane, followed by water vapour, O_3 (*ca*. 500 ppbv) and SO_2 (*ca*. 50 ppbv). A gap of five minutes was left prior to addition of the monoterpene, to allow complete mixing. The reaction was then initiated by addition of the monoterpene (*ca.* 400 ppbv for α-pinene and β-pinene, *ca.* 200 ppbv for limonene), and reagent concentrations followed for roughly 30 - 60 minutes; *ca*. 30 – 90 % of the monoterpene was consumed after this time, dependent on the reaction rate with ozone. Four α-pinene + O_3, five β-pinene + O_3, and five limonene + O_3 experiments, as a function of $[H_2O]$, were performed in total. Each individual run was performed at a constant humidity, with humidity varied to cover the range of $[H_2O] = 0.1 – 19 \times 10^{16}$ molecules cm^{-3}, corresponding to an RH range of 0.1 – 28 % (at 298 K). Measured increases in $[SO_2]$ agreed with measured volumetric additions across the SO_2 and humidity ranges used in the experiments (Newland et al., 2015a).

2.2 Analysis

A range of different SCI are produced from the ozonolysis of each of the three monoterpenes (see Schemes 2 – 4), each with their own distinct chemical behaviour (*i.e.* yields, reaction rates); it is therefore not feasible (from these experiments) to obtain data for each SCI independently; consequently, for analytical purposes we necessarily treat the SCI population in a simplified (lumped) manner – see Section 2.2.2.

SCI are assumed to be formed in the ozonolysis reaction with a yield ϕ (Reaction R1). They can then react with SO_2, with H_2O, with acids formed in the ozonolysis reaction, with other species present, or undergo unimolecular decomposition, under the experimental conditions applied (Reactions R2 – R5). A fraction of the SCI produced reacts with SO_2. This fraction (*f*)

is the loss rate of the SCI to SO_2 ($k_2[SO_2]$) compared to the sum of the total loss processes for the SCI (Equation E1) :

$$f = \frac{k_2[\mathrm{SO_2}]}{k_2[\mathrm{SO_2}] + k_3[\mathrm{H_2O}] + k_d + k_5[\mathrm{acid}] + \mathrm{L}} \quad \text{(E1)}$$

Here, L accounts for the sum of any other chemical loss processes for SCI in the chamber, with the exception of reaction with acids these loss processes are expected to be negligible, as discussed later. After correction for dilution, and neglecting other (non-alkene) chemical sinks for O_3, such as reaction with HO_2 (also produced directly during alkene ozonolysis (Alam et al., 2013; Malkin et al., 2010)), which was indicated through model calculations to account for < 0.5 % of ozone loss under all the experimental conditions, the following equation is derived:

$$\frac{d\mathrm{SO_2}}{d\mathrm{O_3}} = \phi f \quad \text{(E2)}$$

From Equation E2, regression of the loss of ozone (dO_3) against the loss of SO_2 (dSO_2) for an experiment at a given RH determines the product $f\phi$ at a given point in time. This quantity will vary through the experiment as SO_2 is consumed, and other potential SCI co-reactants are produced, as predicted by Equation E1. A smoothed fit was applied to the experimental data for the cumulative consumption of SO_2 and O_3, ΔSO_2 and ΔO_3, (as shown in Figure 2) to determine dSO_2/dO_3 (and hence $f\phi$) at the start of each experiment, for use in Equation E2. The start of each experiment (*i.e.* when $[SO_2]$ ~ 50 ppbv) was used as this corresponds to the greatest rate of production of the SCI, and hence largest experimental signals (*i.e.* greatest O_3 and SO_2 rate of change; greatest precision) and is the point at which the SCI + SO_2 reaction has the greatest magnitude compared with any other potential loss processes for either reactant species (see discussion below).

Other potential fates for SCIs include reaction with ozone (Kjaergaard et al., 2013; Vereecken et al., 2014; Wei et al., 2014; Vereecken et al., 2015; Chang et al., 2018), with other SCI (Su et al., 2014; Vereecken et al., 2014), carbonyl products (Taatjes et al., 2012), acids (Welz et al., 2014), or with the parent alkene (Vereecken et al., 2014; Decker et al., 2017). Sensitivity analyses using the most recent theoretical predictions (Vereecken et al., 2015) indicate that the reaction with ozone is not significant under any of our experimental, accounting for less than 1.5% of SCI loss for *anti*-SCI (based on *anti*-CH_3CHOO) at the lowest RH (worst case)

experiment. Generally, SCI loss to ozone is calculated to be < 1% for all SCI. Summed losses from reaction with SCI (self-reaction), carbonyls and alkenes are likewise calculated to account for < 1 % of the total SCI loss under the experimental conditions applied.

CH_2OO and CH_3CHOO have been shown to react rapidly (k = 1 – 5 × 10^{-10} cm^3 s^{-1}) with formic and acetic acid (Welz et al., 2014). In ozonolysis experiments, Sipilä et al. (2014) determined the relative reaction rate of acetic and formic acids with $(CH_3)_2COO$ (i.e. k_5/k_2) to be roughly three. Organic acid mixing ratios in this work, as measured by FTIR, reached up to a few hundreds of ppbv, suggesting these will likely be a significant SCI sink in our experiments. We have therefore explicitly included reaction with organic acids in our analysis, incorporating the uncertainty arising from the (unknown) acid reaction rate constant, as described in Section 2.2.1.

The water dimer reactions of non-CH_2OO SCI are not considered in our analysis. The effect of the water dimer reaction with C_{10} and C_9 SCI (rather than the monomer) is expected to be minor at the maximum [H_2O] (2 × 10^{17} cm^{-3}) used in these experiments (< 30 % RH). Further, with analogy to the *syn*/*anti*-CH_3CHOO system, for syn-SCI loss to the dimer (and monomer) will not become competitive at the highest [H_2O] used here; for anti-SCI, the water monomer will already be removing the majority of the SCI at the [H_2O] at which the dimer would become a significant loss process, hence the dimer reaction is deemed unimportant. For CH_2OO, the reaction rates with water and the water dimer have been quantified in recent EUPHORE experimental studies, and the values from Newland et al. (2015a) are used in our analysis.

2.2.1 Derivation of $k(SCI+H_2O)/k(SCI+SO_2)$ and $k_d/k(SCI+SO_2)$

As noted above, a range of different SCI are produced from the ozonolysis of the three monoterpenes (see Schemes 2 – 4), each with their own distinct chemical behaviour, which treated individually, introduce too many unknowns (*i.e.* yields, reaction rates) for explicit analysis. Consequently for analytical purposes we treat the SCI population in a simplified (lumped) manner:

Firstly, we use the simplest model possible, assuming that a single SCI is formed in each ozonolysis reaction (Equation E3).

$$\frac{f}{[SO_2]} = \left([SO_2] + \frac{k_3}{k_2}[H_2O] + \frac{k_d}{k_2} + \frac{k_5}{k_2}[\text{acid}] \right)^{-1} \quad \text{(E3)}$$

In a second model, for each monoterpene, the SCI produced are assumed to belong to one of two populations, denoted SCI-A and SCI-B. These two populations are split according to the observation that the decomposition rates and reaction rates with water for the smaller SCI (CH_3CHOO) have been predicted theoretically (Ryzhkov and Ariya, 2004; Kuwata et al., 2010; Anglada et al., 2011) and shown experimentally (Taatjes et al., 2013; Sheps et al., 2014; Newland et al., 2015a) to exhibit a strong dependence on the structure of the molecule. The *syn*-CH_3CHOO conformer, which has the terminal oxygen of the carbonyl oxide moiety in the *syn* position to the methyl group, has been shown to react very slowly with water and to readily decompose, via the hydroperoxide mechanism; whereas the *anti*-CH_3CHOO conformer, with the terminal oxygen of the carbonyl oxide moiety in the *anti*-position to the methyl group, has been shown to react fast with water and is not able to decompose via the hydroperoxide mechanism. Vereecken and Francisco (2012) have shown that all SCI studied theoretically with an alkyl group in the *syn* position have reaction rates with H_2O of $k < 4 \times 10^{-17}$ molecule cm^3 s^{-1} (and for SCI larger than acetone oxide, $k < 8 \times 10^{-18}$ molecule cm^3 s^{-1}).

We thus define two populations, assuming SCI-A (i.e. SCI that exhibit chemical properties of the *anti*-type SCI) to react fast with water and not to undergo unimolecular reactions, and SCI-B (i.e. SCI that exhibit chemical properties of the *syn* type SCI) to not react with water but to undergo unimolecular reactions. This simplification allows us to fit to the measurements using Equations E4 and E5, as shown below. The total SCI yields are determined by our experiments at high SO_2, and the relative yields of SCI-A and SCI-B are determined from fitting to Equation E5. These relative yields are then compared to those predicted from the literature.

In this model, $f = \gamma^A f^A + \gamma^B f^B$, where γ is the fraction of the total SCI yield (i.e. $\gamma^A + \gamma^B = 1$). f^A and f^B are the fractional losses of SCI-A and SCI-B to reaction with SO_2. Adapting Equation E1 to include the two SCI species gives Equation E4, where $k_5[acid]$ accounts for the SCI + acid reaction (see discussion of reaction rate constants below).

$$f = \frac{\gamma^A k_2^A [SO_2]}{k_2^A [SO_2] + k_3 [H_2O] + k_5^A [\text{acid}]} + \frac{\gamma^B k_2^B [SO_2]}{k_2^B [SO_2] + k_d + k_5^B [\text{acid}]} \quad \text{(E4)}$$

Equation E4 can be rearranged to Equation E5 and fitted according to $f/[SO_2]$ derived from the measurements.

$$\frac{f}{[SO_2]} = \frac{\gamma^A}{[SO_2] + \frac{k_3}{k_2^A}[H_2O] + \frac{k_5^A}{k_2^A}[acid]} + \frac{\gamma^B}{[SO_2] + \frac{k_d}{k_2^B} + \frac{k_5^B}{k_2^B}[acid]} \quad \text{(E5)}$$

Using values for γ^A and γ^B from the literature and varying the assumed values of the reaction of SCI with acid (k_5) allows us to determine k_3/k_2^A and k_d/k_2^B.

The assumptions made here allow analysis of a very complex system. However, a key consequence is that the relative rate constants obtained from the analysis presented here are not representative of the elementary reactions of any single specific SCI isomer formed, but rather represent a quantitative ensemble description of the integrated system, under atmospheric boundary layer conditions, which may be appropriate for atmospheric modelling. Additionally our experimental approach cannot determine absolute rate constants (*i.e.* values of k_2, k_3, k_d) in isolation, but is limited to assessing their relative values, measured under atmospheric conditions, which may be placed on an absolute basis through use of an external reference value (here the SCI + SO_2 rate constant).

2.2.2 SCI yield calculation

The value for the total SCI yield of each monoterpene, $\phi_{SCI\text{-}TOT}$, was determined from an experiment performed under dry conditions (RH < 1%) in the presence of excess SO_2 (*ca.* 1000 ppbv), such that SO_2 scavenged the majority of the SCI. From Equation E2, regressing dSO_2 against dO_3 (corrected for chamber dilution), assuming f to be unity (*i.e.* all the SCI produced reacts with SO_2), determines the value of ϕ_{min}, a lower limit to the SCI yield. Figure 1 shows the experimental data, from which ϕ_{min} was derived.

In reality f will be less than one, at experimentally accessible SO_2 levels, as a fraction of the SCI may still react with trace H_2O present, or undergo unimolecular reaction. The actual yield, ϕ_{SCI}, was determined by combining the result from the excess-SO_2 experiment with those from the series of experiments performed at lower SO_2, as a function of $[H_2O]$, to obtain k_3/k_2 and k_d/k_2 (see Section 2.2.1), through an iterative process to determine the single unique value of ϕ_{SCI} which fits both datasets, as described in Newland et al. (2015a), but taking into account the proposed model in this paper of there being two SCI produced. In this model, f =

$\gamma^A f^A + \gamma^B f^B$. Where $f^A = [SO_2] / ([SO_2] + k_3[H_2O]/k_2)$ and $f^B = [SO_2] / ([SO_2] + k_d/k_2)$ – other possible SCI sinks are assumed to be negligible. In these excess-SO_2 experiments, $f^A \sim 1$ but $f_B < 1$ since k_d still represents a significant sink.

γ^A (and hence γ^B, since $\gamma^B = 1 - \gamma^A$) is derived from fitting Equation E4 to the data from the experiments performed at lower SO_2 for a given ϕ. Using a range of ϕ, gives a range of γ. These different values of γ are used with the respective values of ϕ in fitting to Equation E4 to determine values of k_3/k_2 and k_d/k_2.

2.2.3 Experimental uncertainties

The uncertainty in k_3/k_2 was calculated by combining the mean relative errors from the precision associated with the SO_2 and ozone measurements (given in Section 2.1) with the 2σ error and the relative error in φ, using the root of the sum of the squares of these four sources of error. The uncertainty in k_d/k_2 was calculated in the same way.

The uncertainty in φ_{min} was calculated by combining the uncertainty in ΔSO_2 and ΔO_3, as above. The uncertainty in φ was calculated by applying the k_3/k_2 uncertainties and combining these with the uncertainties in φ_{min}, using the root of the sum of the squares.

3 Theoretical calculations

The rovibrational characteristics of all conformers of the CI formed from α-pinene and β-pinene, the transition states for their unimolecular reaction, and for their reaction with H_2O, were characterized quantum chemically, first using the M06-2X/cc-pVDZ level of theory, and subsequently refined at the M06-2X/aug-cc-pVTZ level. To obtain the most accurate barrier heights for reaction, it has been shown (Berndt et al., 2015; Chhantyal-Pun et al., 2017; Fang et al., 2016a, 2016b; Long et al., 2016; Nguyen et al., 2015) that post-CCSD(T) calculations are necessary. Performing such calculations for the SCI discussed in this paper, with up to 14 non-hydrogen atoms, is well outside our computational resources. Instead, we base our predictions on high-level CCSD(T)/aug-cc-pVTZ single point energy calculations, performed for the reactions of nopinone oxides and the most relevant subset of pinonaldehyde oxides. These data are reliable for relative rate estimates, but it remains useful to further improve the absolute barrier height predictions, as described by Vereecken et al. (2017) based on a data set with a large number of systematic calculations on smaller CI, allowing empirical corrections

to estimate the post-CCSD(T) barrier heights. Briefly, they compare rate coefficient calculations against available harmonized experimental and very-high level theoretical kinetic rate predictions, and adjusts the barrier heights by 0.4 to 2.6 kcal mol^{-1} (depending on the base methodology and the reaction type) to obtain best agreement with these benchmark results.

Using the energetic and rovibrational data thus obtained, multi-conformer transition state theory (MC-TST) calculations (Truhlar et al., 1996; Vereecken and Peeters, 2003) were performed to obtain the rate coefficient at 298K at the high pressure limit. All rate predictions incorporate tunnelling corrections using an asymmetric Eckart barrier (Eckart, 1930; Johnston and Heicklen, 1962). For the reaction of CI + H_2O, a pre-reactive complex is postulated at 7 kcal mol^{-1} below the free reactants, while the CI + $(H_2O)_2$ reaction is taken to have a pre-reactive complex of 11 kcal mol^{-1} stability. This pre-reactive complex affects tunnelling corrections; it is assumed that this pre-reactive complex is always in equilibrium with the free reactants.

In view of the high number of rotamers and the resulting computational cost, only a single limonene-derived CI isomer was studied, where the TS for the CI + H_2O reaction was analyzed at the M06-2X/cc-pVDZ level of theory with only a partial conformational analysis; a limited number of the energetically most stable TS conformers thus discovered were re-optimized at the M06-2X/aug-cc-pVTZ level of theory. These data will only be used for qualitative assessments. However, we apply the structure-activity relationships (SARs) presented by Vereecken et al. (Vereecken et al., 2017) to obtain an estimate of the rate coefficients, and assess the role of the individual SCI isomers in limonene ozonolysis.

All quantum chemical calculations were performed using Gaussian-09 (Frisch et al., 2010).

4 GEOS-Chem Model Simulation

The global chemical transport model GEOS-Chem (v9-02, www.geos-chem.org, Bey et al., 2002) is used to explore the spatial and temporal variability of the atmospheric impacts of the experimentally derived chemistry. The model includes HOx-NOx-VOC-O_3-BrOx chemistry (Mao et al., 2010; Parrella et al., 2012) and a mass-based aerosol scheme. Biogenic monoterpene emissions are taken from the Model of Emissions of Gases and Aerosols from Nature (MEGAN) v2.1 inventory (Guenther et al., 2006; 2012). Transport is driven by assimilated meteorology (GEOS-5) from NASA's Global Modelling and Assimilation Office

(GMAO). The model is run at 4°×5° resolution, with the second year (2005) used for analysis and first year discarded as spin up.

In this study, the standard simulation was expanded to include emissions of seven monoterpene species (α-pinene, β-pinene, limonene, myrcene, ocimene, carene, and sabinene) from MEGAN v2.1. The ozonolysis scheme for each monoterpene, detailed in Section 7.1, considers the formation of one or two types of SCI, and their subsequent reaction with SO_2, H_2O, or unimolecular decomposition. The reaction rates of the monoterpenes with OH, O_3 and NO_3 are detailed in Table S1.

5 Experimental Results

5.1 SCI Yield

Figure 1 shows the lower limit to the SCI yield, ϕ_{min}, for the three monoterpenes, determined from fitting Equation E5 to the experimental data. This gives values of 0.16 (± 0.01) for α-pinene, 0.53 (± 0.01) for β-pinene and 0.20 (± 0.01) for limonene. These ϕ_{min} values were then corrected as described in Section 2.2.2 using the k_3/k_2 and k_d/k_2 values determined from the measurements shown in Figures 3 – 5 using Equation E4. The corrected yields, ϕ_{SCI}, are 0.19 (± 0.01) for α-pinene, 0.60 (± 0.03) for β-pinene and 0.23 (± 0.01) for limonene. Uncertainties are ± 2σ, and represent the combined systematic (estimated measurement uncertainty) and precision components. Literature yields for SCI production from monoterpene ozonolysis are summarised in Table 1.

The value derived for the total SCI yield from α-pinene in this work of 0.19 agrees, within the uncertainties, with the value of 0.15 (± 0.07) reported by Sipilä et al. (2014) and the value of 0.20 applied in the MCMv3.3.1.

The total SCI yield from β-pinene derived in this work, 0.60, agrees reasonably well with the recent experimental work of Ahrens et al. (2014) who derived a total SCI yield of 0.50 (0.40 for the sum of CI-1 and CI-2 and 0.10 for CH_2OO, which is assumed to be formed almost completely stabilised). The MCMv3.3.1 applies a total SCI yield of 0.25, of which 0.10 is a C9-CI and 0.15 is CH_2OO. Earlier studies also tended to derive lower total SCI yields ranging from 0.25 – 0.27 (Hasson et al., 2001; Hatakeyama et al., 1984).

The total SCI yield from limonene derived in this work, 0.23 (± 0.01) agrees with the recently determined yield from Sipilä et al. (2014) of 0.27 (± 0.12). Leungsakul et al. (2005) derived a somewhat higher yield of 0.34, while the MCMv3.3.1 applies a lower yield of 0.135.

5.2 $k_3(SCI+H_2O)/k_2(SCI+SO_2)$ and $k_d/k_2(SCI+SO_2)$ Analysis

Figure 2 shows the loss of SO_2 as ozone is consumed by reaction with the monoterpene for each of the three systems. Box modelling results suggest that > 99 % of this SO_2 removal is caused by reaction with SCI produced in the alkene-ozone reaction (rather than e.g. reaction with OH, which is scavenged by cyclohexane). When the experiments are repeated at higher relative humidity, the rate of loss of SO_2 decreases. This is as expected from Equation E1 and suggests that there is competition between SO_2 and H_2O for reaction with the SCI produced, in agreement with observations of smaller SCI, which demonstrate the same competition under atmospherically relevant conditions (Newland et al., 2015a; Newland et al., 2015b).

However, as the relative humidity is increased further, the SO_2 loss does not fall to (near) zero as would be expected from Equation E1. This suggests that at high [H_2O] the amount of SO_2 loss becomes less sensitive to [H_2O]. This is most likely due to there being at least two chemically distinct SCI species present. This behaviour was previously observed for CH_3CHOO by Newland et al. (2015a) and fits with the current understanding that the reactivity of SCI is structure dependent.

To recap Section 2.2.1, the analysis presented here considers two models to fit the observations. The first of these (Equation E3) assumes the formation of a single SCI species, which, in addition to reacting with SO_2, can react with water, undergo unimolecular reaction or react with acid. It is clearly evident from Figures 3 – 5 that this model does not give a good fit to the observations for any of the monoterpene systems studied. Therefore, the results from this (single SCI) approach are not discussed explicitly hereafter. The second of the models (Equation E5) assumes the formation of two lumped, chemically distinct, populations of SCI, denoted SCI-A and SCI-B. SCI-A is assumed to react fast with H_2O and to have minimal decomposition. Conversely, SCI-B is assumed to have a negligible reaction with water under the experimental conditions applied but to undergo rearrangement via a VHP. We use a least-squares fit of Equation E5 to the data to determine the values of k_3/k_2 and k_d/k_2. This approach fits the data well (Figures 3 - 5) for all 3 monoterpenes and represents the overall attributes of

the SCI formed - but as noted, does not represent an explicit determination of individual conformer-dependent rate constants.

5.2.1 α-pinene

The α-pinene system is sensitive to water vapour at the low H_2O range, with the SO_2 loss falling dramatically when the RH is increased from 0.1 to 2.5 % (Figure 2). However, at higher RH the SO_2 loss appears to be rather insensitive to $[H_2O]$.

CI-1 can be formed in either a *syn* (1a) or *anti* (1b) configuration, whereas both CI-2 conformers formed are in a *syn* configuration (see Scheme 2). For one of the two conformers of CI-2 (CI-2b), the hydrogen atom available for abstraction by the terminal oxygen of the carbonyl oxide group is attached to the carbon on the four-membered ring. This has been shown in the β-pinene system to make a large difference with respect to the ability of the hydrogen to be abstracted and to undergo the VHP mechanism (Rickard et al., 1999; Nguyen et al., 2009). This therefore suggests that CI-2b may exhibit characteristics of both SCI-A and SCI-B. Ma et al. (2008) infer a probable equal yield of the two basic CI structures. This would suggest a relative yield for SCI-A of 0.25 – 0.50 (depending on the precise nature of CI-2b). Fitting Equation E4 to the data and allowing lambda to vary determines values of γ^A = 0.40 and γ^B = 0.60 (Figure 3).

In Figure 3, Equation E4 is fitted to the α-pinene measurements, assuming $k(\text{SCI+acid})/k(\text{SCI+SO}_2) = 0$. This derives a minimum value for $k(\text{SCI-A+H}_2\text{O})/k(\text{SCI-A+SO}_2)$, the water dependent fraction of the SCI, and a maximum value for $k(\text{decomposition:SCI-B})/k(\text{SCI-B+SO}_2)$, the water independent fraction of the SCI. The kinetic parameters derived from the fitting are displayed in Table 2.

Figure 6 shows the variation of the derived k_3/k_2 and k_d/k_2 values as the ratio k_5/k_2, $k(\text{SCI+acid})/k(\text{SCI+SO}_2)$, is varied from zero to one. The derived k_3/k_2 increases by about 40 % from 1.4 (± 0.34) × 10^{-3} to 2.0 (± 0.49) × 10^{-3}. The derived k_d/k_2 value decreases, again by about 40 %, from 8.2 (± 1.5) × 10^{12} cm^{-3} to 5.1 (± 0.93) × 10^{12} cm^{-3}.

The derived limits to the relative rate constants can be put on an absolute scale using the $k(\text{SCI+SO}_2)$ values for CH_3CHOO from Sheps et al. (2014) for the *syn* and *anti* conformers. These are, *syn*: 2.9 × 10^{-11} cm^3 s^{-1} and *anti*: 2.2 × 10^{-10} cm^3 s^{-1}. The *syn* rate constant is applied to the derived $k(\text{decomposition:SCI-B})/k(\text{SCI-B+SO}_2)$ value and the *anti* rate constant to the $k(\text{SCI-A+H}_2\text{O})/k(\text{SCI-A+SO}_2)$ value. It should be noted that the k_2 values are for quite

different SCI to those formed in this study and to our knowledge no structure specific k(SCI+SO_2) have been reported for monoterpene derived SCI, though Ahrens et al. (2014) determine an average $k_2 \sim 4 \times 10^{-11}$ cm^3 s^{-1} for SCI derived from β-pinene, i.e. a value within an order of magnitude of those determined for the smaller SCI CH_2OO, CH_3CHOO and $(CH_3)_2COO$ (e.g. Welz et al., 2012; Taatjes et al., 2013; Sheps et al., 2014; Huang et al., 2015). Using the Sheps et al. (2014) values yields k(SCI-A+H_2O) > 3.1 (± 0.75) × 10^{-13} cm^3 s^{-1} and k(decomposition:SCI-B) < 240 (± 44) s^{-1} (using the values derived for k(SCI-A+acid)/k(SCI-A+SO_2) = 0). This k_3 value is an order of magnitude larger than the rate constants determined for the smaller *anti*-CH_3CHOO in the direct studies of Sheps et al. (2014) (2.4 × 10^{-14} cm^3 s^{-1}) and Taatjes et al. (2013) (1.0 × 10^{-14} cm^3 s^{-1}). The decomposition value derived for SCI-B is of the same order of magnitude as that for *syn*-CH_3CHOO (348 ± 332 s^{-1}) and $(CH_3)_2COO$ (819 ± 190 s^{-1}) from Newland et al., (2015a) (using updated direct measurement values of k_2 from Sheps et al. (2014) and Huang et al. (2015) for *syn*-CH_3CHOO and $(CH_3)_2COO$ respectively) and within the range from the recent paper by Smith et al. (2016) which derives a decomposition rate for $(CH_3)_2COO$ of 269 (± 82) s^{-1} at 283 K increasing to 916 (± 56) s^{-1} at 323 K.

Sipilä et al. (2014) applied a single-SCI analysis approach to the formation of H_2SO_4 from SO_2 oxidation in the presence of the α-pinene ozonolysis system. They determined that for α-pinene, $k_d >> k$(SCI+H_2O)[H_2O] for [H_2O] < 2.9 × 10^{17} cm^{-3}, i.e. that the fate of SCI formed in the system is rather insensitive to [H_2O]. Across the [SO_2] and RH ranges used in their study, the results obtained here would indicate H_2O to always be the dominant sink for SCI-A, i.e. the fact that Sipilä et al. (2014) see similar H_2SO_4 production across the RH range in their study is consistent with these results.

5.2.2 β-pinene

Two recent studies (Nguyen et al., 2009; Ahrens et al., 2014) have suggested yields of the two C_9-CI (CI-3 and CI-4, see Scheme 3) obtained from β-pinene ozonolysis to be roughly equal. In these studies Ahrens et al. (2014) assume a CH_2OO yield of 0.10 while Nguyen et al. (2009) determine theoretically the yield of CH_2OO to be 0.05. Another theoretical study (Zhang and Zhang, 2005) predicted a CH_2OO yield of 0.08. In experimental studies, Winterhalter et al. (2000) determined the CH_2OO yield to be 0.16 (± 0.04) from measuring

the nopinone yield and assuming it to be entirely a primary ozonolysis product (i.e. the co-product of CH_2OO formation) and Ma and Marston (2008) determine a summed contribution of 84 % (± 0.03) for the two C_9-CI (i.e. a 16 % CH_2OO yield). The theoretical studies are somewhat lower than the experimental but Nguyen et al. (2009) note that CI-4 is likely to form additional nopinone in bimolecular reactions. The CH_2OO is assumed to all be formed stabilised (e.g. Nguyen et al. 2009).

SCI-3 is expected to undergo unimolecular reactions at least an order of magnitude faster than SCI-4 (Nguyen et al., 2009; Ahrens et al., 2014). The reaction of SCI-3 with water is expected to be slow based on the calculations presented in Table 4, with a pseudo first order reaction rate of 0.3 s^{-1} at the highest [H_2O] used here, 2×10^{17} cm^{-3}, 298 K, whereas the water reaction with SCI-4 is expected to be considerably faster with a pseudo first order reaction rate of 85 s^{-1} at [H_2O] = 2×10^{17} cm^{-3}, 298 K. This reaction would thus be expected to be competitive with reaction with SO_2 for SCI-4 under the experimental conditions employed. This is in agreement with the observations of Ma and Marston (2008), which show a clear dependence of nopinone formation on RH (presumed to be formed from SCI + H_2O). Fitting Equation E4 to the data determines values of $\gamma^A = 0.41$ and $\gamma^B = 0.59$ (Figure 4).

Using these values, and assuming k(SCI+acid)/k(SCI+SO_2) = 0, yields a k(SCI-A+H_2O)/k(SCI-A+SO_2) value of > 1.0 (± 0.27) × 10^{-4} and a k(decomposition:SCI-B)/k(SCI-B+SO_2) value of < 6.0 (± 1.3) × 10^{12} cm^{-3} (Table 2).

As shown in Figure 6, increasing k_5/k_2, k(SCI+acid)/k(SCI+SO_2), from zero to one, decreases the derived k_d/k_2 from 6.0 (± 1.3) × 10^{12} cm^{-3} to 1.8 (± 0.39) × 10^{12} cm^{-3}. The derived k_3/k_2 increases by a factor of four from 1.0 (± 0.27) × 10^{-4} to 3.7 (± 1.0) × 10^{-4}.

These values can be put on an absolute scale (using the values derived above for $k_5/k_2 = 0$). For SCI-A, k(SCI+SO_2) is taken as the experimentally determined value of 4×10^{-11} cm^3 s^{-1} from Ahrens et al. (2014). For SCI-B, the *syn*-CH_3CHOO k(SCI+SO_2) value determined by Sheps et al. (2014) is used. This gives values of k(SCI-A+H_2O) > 4×10^{-15} (± 1) cm^3 s^{-1} and k(decomposition:SCI-B) < 170 (± 38) s^{-1}.

5.2.3 Limonene

For the limonene measurements presented in Figure 2, ($d$$SO_2$/$d$$O_3$)/$dt$ appears to be non-linear, with a jump in $d$$SO_2$/$d$$O_3$ between 120 and 150 ppbv of ozone consumed. This is most evident in the two lowest RH runs (0.2 and 2.0 %). Limonene is the fastest reacting of the

systems presented here, with the alkene reaction having consumed 100 ppbv of ozone within the first five minutes. The limonene sample required about five minutes of heating before the entire sample was volatized and injected into the chamber. This therefore may account for the apparent non-linear nature of $d[SO_2]/d[O_3]$ in Figure 2.

The SO_2 loss in the limonene-ozone system is less affected by increasing H_2O than for either α or β-pinene (Figure 5), with the values of $f/[SO_2]$ (y-axis) varying by roughly a factor of two over the RH range applied compared to more than a factor of three variation for the other two systems. Hence it might be expected that there is little formation of H_2O dependent SCI or that it has a rather slow reaction rate with water.

Fitting Equation E4 to the data determines values of $\gamma^A = 0.22$ and $\gamma^B = 0.78$ (Figure 5). This is broadly in line with the ratio recommended in the MCMv3.3.1 of 0.27:0.73, and with that proposed in Leungsakul et al. (2005) who use a CI-A:CI-B ratio of 0.35:0.65, but also include some stabilisation of CH_2OO and C_9-CI from ozone reaction at the exo-cyclic bond. This yields a $k(\text{SCI-A}+H_2O)/k(\text{SCI-A}+SO_2)$ value of $< 3.5\ (\pm 0.20) \times 10^{-5}$ and a $k(\text{decomposition:SCI-B})/k(\text{SCI-B}+SO_2)$ value of $> 4.5\ (\pm 0.10) \times 10^{12}$ cm^{-3}.

Figure 6 shows that the derived k_d/k_2 increases by about 7 % as $k(\text{SCI+acid})/k(\text{SCI}+SO_2)$ ranges from 0.0 to 0.8. The derived k_3/k_2 becomes negative at $k(\text{SCI+acid})/k(\text{SCI}+SO_2) > 0.8$, putting an upper limit on this ratio, i.e. $k_5/k_2 < 0.8$, for the limonene system.

Putting these values on an absolute scale (using the values derived for $k_5/k_2 = 0$), using the CH_3CHOO *syn* and *anti* $k(\text{SCI}+SO_2)$ determined by Sheps et al. (2014), yields values of $< 7.7\ (\pm 0.60) \times 10^{-15}$ cm^3 s^{-1} and $> 130\ (\pm 3)$ s^{-1} for k_3 and k_d respectively. These values are similar to those derived for the SCI-A and SCI-B formed from β-pinene. The k_3 value is a factor of three smaller than that determined by Sheps et al. (2014) for $k_3(\textit{anti}\text{-}CH_3CHOO+H_2O)$, 2.4×10^{-14} cm^3 s^{-1}.

Sipilä et al. (2014) applied a single-SCI analysis approach to the formation of H_2SO_4 from SO_2 oxidation by the limonene ozonolysis system and determined that, similarly to α-pinene, $k(\text{decomp.}) >> k(\text{SCI}+H_2O)[H_2O]$ for $[H_2O] < 2.9 \times 10^{17}$ cm^{-3}, i.e. that the system is rather insensitive to $[H_2O]$. Our data are consistent with the limonene system being less sensitive to $[H_2O]$ than the SCI populations derived from the other two monoterpenes reported here.

5.2.4 Experimental Summary

The reaction rates of SCI-A (i.e. SCI that exhibit chemical properties of the *anti*-type SCI) derived from the three different monoterpenes with water range from < 0.8 to > 31 × 10^{-14} cm^3 s^{-1}, broadly in line with the derived rates of Sheps et al. (2014) for *anti*-CH_3CHOO of 2.4 × 10^{-14} cm^3 s^{-1}. The decomposition rates of SCI-B (i.e. SCI that exhibit chemical properties of the *syn*-type SCI) are on the order of 100 - 250 s^{-1}. This is in line with those derived for *syn*-CH_3CHOO from *cis* and *trans*-but-2-ene ozonolysis and $(CH_3)_2COO$ by Newland et al. (2015a) of 348 (± 332) s^{-1} and 819 (± 190) s^{-1} respectively (assuming k(*syn*-$CH_3CHOO+SO_2$) = 2.9 × 10^{-11} cm^3 s^{-1} (Sheps et al., 2014) and $k((CH_3)_2COO+SO_2)$ = 2.9 × 10^{-10} cm^3 s^{-1} (Huang et al., 2015)) and recent results from Smith et al. (2016) of 269 – 916 s^{-1} (strongly dependent on temperature) for $(CH_3)_2COO$ decomposition. In this work we only derive relative rates, but the similarity of the k_3 and k_d values derived when the k_2 values for *syn* and *anti*-CH_3CHOO from Sheps et al. (2014) are applied is consistent with the recent work of Ahrens et al. (2014), suggesting that large SCI, derived from monoterpenes, demonstrate a similar reactivity towards SO_2 as smaller SCI. One uncertainty in the derivation of the kinetics presented herein is the reactions of the SCI produced with organic acids. These acids were present in the experiments (owing to formation in the monoterpene ozonolysis reactions themselves) at levels which may have been a competitive sink for the SCI.

6 Theoretical results and comparison to experiments

The theoretically predicted rate coefficients for unimolecular reactions of the monoterpene SCI are listed in Table 3, while those for the reaction with H_2O are listed in Table 4. These data can be compared against the experimental data obtained in this work.

6.1.1 α-pinene

The theory-based rate coefficients show one pinonaldehyde oxide, CI-1b, with a rate of reaction with water that is significantly faster than the remaining α-pinene-derived CI. Comparing this rate to the experimental data suggests that CI-1b corresponds to SCI-A, with matching rate coefficients within an order of magnitude, i.e. within the expected uncertainty. We thus deduce that SCI-A is CI-1b. The remaining pinonaldehyde oxides, CI-1a, CI-2a and CI-2b, react predominantly through unimolecular reactions, where theory-based rate coefficients range from 60 to 600 s^{-1}, all within a factor of 4 of the experimentally derived

population-averaged rate of 240 ± 44 s^{-1}, i.e. matching within the uncertainty margins. The unimolecular rate coefficients of this set of CI are sufficiently close that it is not feasible to separate these in the experimental data, so we can only conclude that SCI-B in the α-pinene ozonolysis experiments may consist of a mixture of C-1a, CI-2a and CI-2b.

6.1.2 β-pinene

The theoretical analysis for nopinone oxides shows one isomer, SCI-4, that has a fast rate of reaction with water, but a slow unimolecular isomerisation, while the other isomer, SCI-3, shows a fast unimolecular decomposition. These can thus be unequivocally equated to the experimentally obtained SCI-A and SCI-B, respectively, inasmuch as the yield of CH_2OO is minor. The predicted rate coefficients are within the expected uncertainty intervals of the theoretical data, a factor of 5 for the unimolecular rates, and an order of magnitude for the reaction with H_2O.

The experimental rate measurements are defined relative to the reaction rate with SO_2; the value adopted for the k(SCI+SO_2) reaction therefore influences the derived rate coefficient values. Ahrens et al. (2014) directly measured the SO_2 rate coefficient of the longest-lived SCI (SCI-4) to be ~ 4×10^{-11} cm^3 s^{-1}, but for SCI-3 we assume a similar rate coefficient as *syn*-CH_3CHOO + SO_2 determined by Sheps et al. (2014) of 2.9×10^{-11} cm^3 s^{-1}. Nopinone oxides are bicyclic compounds, with a bulky dimethyl-substituted 4-membered ring adjacent to the carbonyl oxide moiety. To examine the potential impact of steric hindrance on the SCI + SO_2 reaction, we characterized all sulfur-substituted secondary ozonides (S-SOZ) formed in this reaction (Kuwata et al., 2015; Vereecken et al., 2012). We find that the tri-cyclic S-SOZ shows very little interaction between the sulfur-bearing ring and the β-pinene substituents, and little change in ring strain. The energies of the S-SOZ adducts relative to the SCI + SO_2 reactants thus remains very similar to that of CH_2OO, CH_3CHOO or $(CH_3)_2COO$, confirming the quality of our selection of reference rate coefficients.

6.1.3 Limonene

Of the six non-CH_2OO CI formed in limonene ozonolysis, CI-5b was predicted to have a fast reaction rate with H_2O; its oxide substitution patterns is similar to pinonaldehyde oxide CI-1b. The SAR-predicted rate coefficient of CI-5b + H_2O is within a factor of 2 of the experimentally derived k_3 value for SCI-A, such that we can equate SCI-A to CI-5b with

confidence. The SCI-B set of Criegee intermediates then contains the summed population of the remaining five CI, all of which react slowly with H_2O. The SAR-predicted unimolecular decay rate coefficients range from 15 to 700 s^{-1}, all within a factor of 9 of the experimentally obtained k_d = 130 s^{-1}; it should be noted that for limonene-derived CI, no explicit theoretical calculations are available, and the SAR-predictions carry a somewhat larger uncertainty. We have performed an exhaustive characterisation of the conformers of CI-5b. The most stable conformers show an internal complex formation between the oxide moiety and the carbonyl group, similar to those characterized for the bimolecular reaction of CI with carbonyl compounds (Jalan et al., 2013; Wei et al., 2015). The theoretical study by Jiang et al. (2013) on limonene ozonolysis appears to have omitted internal rotation and cannot be compared directly. It seems likely that the limonene-derived CI can thus easily undergo internal SOZ formation, which is thought (Vereecken and Francisco, 2012) to be entropically unfavourable, but to have a low barrier to reaction. For α-pinene, a similar internal complex formation and SOZ ring closure is not as favourable due to the geometric limitations enforced by the 4-membered ring.

A large number of transition state conformers for CI-5b + H_2O were characterized, though no exhaustive search was completed. The energetically most favourable structures show interaction between the carbonyl group, and the H_2O co-reactant as it adds onto the carbonyl oxide moiety. Similar stabilising interactions between the carbonyl moiety and the carbonyl oxide moiety were reported recently in cyclohexene-derived CI (Berndt et al., 2017). This interaction thus lowers the barrier to reaction though it is currently unclear whether it enhances the reaction rate compared to e.g. the α-pinene-derived CI-1b, as these hydrogen-bonded structures are entropically not very favourable. The intra-molecular interactions with heterosubstituents could be investigated in future work.

7 Global modelling study

7.1 SCI Chemistry

A global atmospheric modelling study was performed using the GEOS-Chem chemical transport model (as described in Section 4) to examine the global monoterpene derived SCI budget and the contribution of these SCI to gas-phase SO_2 oxidation. The existing chemistry scheme in the model is supplemented with monoterpene SCI chemistry based on the

experimental results described in Section 5 and in Table 5. It should be noted here that this modelling study focuses on the chemical impacts of monoterpene SCI formed from ozonolysis reactions only. No chemistry for other SCIs derived from isoprene and/or other (smaller) alkenes are incorporated in the adapted model chemical scheme used.

The monoterpene emissions in GEOS-Chem are taken from MEGAN v2.1 (Guenther et al., 2012). The scheme emits seven monoterpenes: α-pinene, β-pinene, limonene, myrcene, ocimene, 3-carene, and sabinene. The monoterpenes are oxidised within the model by OH, NO_3 and O_3 at rates shown in Table S1. Reaction with O_3 leads to the production of monoterpene specific SCI. Reactions with OH and NO_3 does not lead to the formation of any products, with the reactions only acting as a sink for the monoterpene and the respective oxidant. The SCI yields from the ozonolysis of α-pinene, β-pinene, and limonene are derived from the experimental work presented here. SCI from each monoterpene are split in to SCI-A and SCI-B as defined in previous sections. For the other four monoterpenes emitted, the SCI yields, and kinetics are derived based on similarity of structure to one of the species studied here or previously in the literature. The main SCI produced in the ozonolysis of myrcene and ocimene are expected to be acetone oxide ($(CH_3)_2COO$) or 4-vinyl-5-hexenal oxide ($CH_2CHC(CH_2)CH_2CH_2CHOO$), since ozone has been suggested to react predominantly at the internal double bond (~97 % for myrcene, ~90% for ocimene (Baker et al., 2004)). The SCI yield is taken to be 0.30, similar to that of $(CH_3)_2COO$ from 2,3-dimethyl-but-2-ene ozonolysis (Newland et al., 2015a). However, this may be an underestimate since it has been predicted that stabilisation of small CI increases with an increasing size of carbonyl co-product, as this co-product can take more of the nascent energy of the primary ozonide on decomposition due to a greater number of degrees of freedom available (Nguyen et al., 2009, Newland et al., 2015b). Sabinene is a bicyclic monoterpene with an external double bond and hence is treated like β-pinene. This assumption is backed up by recent theoretical work (Wang and Wang, 2017), who predict similar behaviour of sabinene derived SCI to the predicted behaviour of β-pinene SCI by Nguyen et al. (2009a). They predict a SCI yield between 24 % - 64 %. 3-carene is a bicyclic monoterpene with an internal double bond and is treated like α-pinene.

7.2 Modelling Results

Figure 7 shows the annually averaged total SCI burden from monoterpene ozonolysis in the surface layer in the GEOS-Chem simulation. A number of interesting features are apparent from this figure and the associated information given in Table 6:

(i) The highest annually averaged monoterpene SCI concentrations are found above tropical forests.

(ii) Peak anually averaged monoterpene SCI concentrations are ~ 1.4×10^4 cm^{-3}.

(iii) > 97 % of the total monoterpene SCI burden is SCI-B.

Annual global monoterpene emissions are dominated by the tropics (Figure S1), accounting for > 90 % during the northern hemisphere winter months (November – April) and 70 % even during the peak emissions from the northern boreal region during June and July (Sindelarova et al., 2014). Despite annually averaged surface ozone mixing ratios being roughly a factor of 2 higher in the northern mid-high latitudes, monoterpene SCI production is still dominated by the tropics. Annually averaged surface monoterpene SCI concentrations across the northern boreal regions are < 2×10^3 cm^{-3}; during the summer months (JJA) this value rises to 2 – 5 × 10^3 cm^{-3}.

More than 97 % of the total monoterpene derived SCI are SCI-B (Table 6). This is because typical water vapour concentrations in the tropics are > 5.0×10^{17} cm^{-3}. This gives SCI-A removal rates (i.e. $k_3[H_2O]$) of 2×10^3 – 1.5×10^5 s^{-1}, whereas removal rates of SCI-B to unimolecular reactions have been determined here to be 1 – 3 orders of magnitude slower, on the order of 100 - 250 s^{-1}. Since the loss of SCI-B is independent of temperature in the model, the highest SCI-B concentrations would be expected to be located in the regions of highest SCI-B production. Recent experimental studies (Smith et al., 2016) have demonstrated a strong temperature dependence for the unimolecular decomposition rate of $(CH_3)_2COO$ between 283 and 323 K (269 – 916 s^{-1}). Therefore, it may be that in reality there would be some geographical variation in the rate of unimolecular loss.

The monoterpene SCI-A + H_2O reactions are expected to lead to high yields of both large (e.g. Ma et al., 2008; Ma and Marston, 2008) and small (measured in high yield in the experiments presented here) organic acids.

Figure 8 shows the seasonal removal of SO_2 by reaction with monoterpene derived SCI, as a percentage of total gas-phase SO_2 oxidation in the surface layer. Monoterpene SCI are most

important (relative to OH) for SO_2 oxidation over tropical forests, where they account for up to 60 % of the local gas-phase SO_2 removal during DJF and MAM in some regions. The reasons for this are two-fold: firstly, the highest modelled monoterpene SCI concentrations are found in these regions (Figure 7); but additionally, OH concentrations in the model are low over these areas (Figure S2). Historically there has been discrepancies between modelled and observed OH concentrations over tropical forests, with models appearing to under-predict [OH] by up to a factor of ten (e.g. Lelieveld et al., 2008). It was proposed that this was due to missing sources of OH recycling during isoprene oxidation. During recent years there have been advances in our understanding of isoprene chemistry. GEOS-Chem v-09, used here, includes an isoprene OH recycling scheme largely based on Paulot et al. (2009a, 2009b), with updates from Peeters et al. (2009), Peeters and Müller (2010), and Crounse et al. (2011; 2012), and evaluated in Mao et al. (2013). However, more recent experimental and theoretical work is not yet included.

Annually, monoterpene SCI oxidation accounts for 1.2 % of the gas-phase SO_2 oxidation in the terrestrial tropics. This accounts for the removal of 2.9 Gg of SO_2. Across the northern boreal forests, monoterpene SCI contribute 0.7 % to gas-phase SO_2 removal annually, removing 0.8 Gg of SO_2. Globally, throughout the whole atmosphere, monoterpene SCI account for only 0.5 % of gas-phase SO_2 removal, removing 8.1 Gg of SO_2 annually.

It is noted that MEGAN does not contain oceanic monoterpene emissions, which may increase the global importance of SCI for gas-phase SO_2 removal. Luo and Yu (2010) determined annual global oceanic α-pinene emissions to be 29.5 TgC using a top-down approach, with only 0.013 (Luo and Yu, 2010) – 0.26 (Hackenberg et al., 2017) TgC estimated using a range of bottom-up approaches; clearly there are large uncertainties in oceanic monoterpene emissions. At the upper end of this range they could potentially provide a similar contribution to SCI production and subsequent SO_2 oxidation as monoterpenes emitted from the terrestrial biosphere. SCI production more generally could be further amplified by sources such as marine-derived alkyl iodine photolysis.

Blitz et al. (2017) recently calculated a revised SO_2 + OH reaction rate (k_1 (1 bar N_2) (298 K) = 5.8×10^{-13} cm^3 s^{-1}), based on experimental work and a master equation analysis, which is ~ 40 % lower than the rate given in the most recent JPL data evaluation (Burkholder et al., 2015) ((k_1 (1 bar N_2) (298 K) = 9.5×10^{-13} cm^3 s^{-1}), which is used in the GEOS-Chem model simulation. Figure S3 shows the increased influence of monoterpene derived SCI on gas-

phase SO_2 oxidation if the alternative SO_2 + OH rate is used. This increased the impact of monoterpene SCI to up to 67 % of gas-phase SO_2 removal in regions of the tropical forests during DJF and MAM, with the contribution of monoterpene SCI to global gas-phase SO_2 oxidation increasing to 0.7 %.

While certain monoterpenes appear to be more important than others with regard to the production of SCI which will oxidise SO_2, these results are sensitive to the kinetics used and the assumptions made for the monoterpenes not studied experimentally here. Hence we do not attempt to draw any conclusions about the relative importance of each monoterpene from the modelling. Clearly the most important monoterpenes will be those with high yields of SCI-B, particularly if those SCI-B have a structure that hinders unimolecular decomposition (such as certain β-pinene derived SCI).

8 Conclusions

We report results from an integrated experimental (simulation chamber), theoretical (quantum chemical) and modelling (global chemistry-transport simulation) study of the impacts of monoterpene ozonolysis reactions on stabilised Criegee intermediate (SCI) formation and SO_2 oxidation. The ozonolysis of the monoterpenes α-pinene, β-pinene and limonene have been shown to produce a structurally diverse range of chemically distinct SCIs, with some showing limited sensitivity to / reaction with water vapour under near-atmospheric humidity levels. A multi-component system is required to explain the experimentally observed SO_2 removal kinetics. A two-body model system based on the assumption of a fraction of the SCI produced being reactive towards water (SCI-A; potentially contributing to the significant formation of a range of organic acids in the atmosphere), and a fraction being relatively unreactive towards water (SCI-B), analogous to the structural dependencies observed for the simpler CH_3CHOO SCI system, has been shown to describe the observed kinetic data reasonably well for all the monoterpene systems investigated, and may form a computationally affordable and conceptually accessible basis for the description of this chemistry within atmospheric models. Moreover such an approach is required to accurately predict SCI concentrations, which will be underestimated if a simple average of the properties of the two different SCI classes is used. The atmospheric fate of SCI-B produced from the monoterpenes studied here will be controlled by their removal by unimolecular decomposition. In this work, we have experimentally determined the monoterpene SCI-B decomposition rate to be between 100 and 250 s^{-1}. This has significant implications for the role of monoterpene derived SCI as oxidants

in the atmosphere. The fate of SCI-A will be reaction with water or the water dimer, likely leading to the production of a range of organic acids.

A theory-based analysis of the kinetics of the SCI formed from α-pinene, β-pinene ozonolysis has also been performed, which complements the experimental work. The identification of the likely SCI-A and SCI-B populations and the derived kinetics agree with experimental observations within the respective uncertainties.

A modelling study using the GEOS-Chem global 3-D chemical transport model supplemented with the chemical kinetics elucidated in this work suggests that the global monoterpene derived SCI burden will be dominated (> 97%) by SCI-B. The highest annually averaged SCI concentrations are found in the tropics, with seasonally averaged monoterpene SCI concentrations up to 1.4×10^4 cm^{-3} owing to large monoterpene emissions. Across the boreal forest, average SCI concentrations reach between $3 - 5 \times 10^3$ cm^{-3} during the northern hemisphere summer. Oxidation of SO_2 by monoterpene SCI is shown to also be most important in the tropics. While oxidation by SCI contributes < 1% to gas-phase SO_2 oxidation globally, over tropical forests this can rise to up to 60 % at certain times of the year. Monoterpene SCI driven SO_2 oxidation will increase the production of sulfate aerosol – affecting atmospheric radiation transfer, and hence climate; and reduce the atmospheric lifetime and hence transport of SO_2. These effects will be substantial in areas where monoterpene emissions are significant, in particular over the Amazon, Central Africa and SE Asian rainforests.

Data Availability

Experimental data will be made available in the Eurochamp database (www.eurochamp.org) from the H2020 EUROCHAMP2020 project, GA nº730997

Acknowledgements

The assistance of the EUPHORE staff is gratefully acknowledged., Salim Alam, Marie Camredon and Stephanie La are thanked for helpful discussions. This work was funded by EU FP7 EUROCHAMP 2 Transnational Access activity (E2-2012-05-28-0077) and the UK NERC Projects (NE/K005448/1, Reactions of Stabilised Criegee Intermediates in the Atmosphere: Implications for Tropospheric Composition & Climate) and (NE/M013448/1,

Mechanisms for Atmospheric chemistry: GeneratioN, Interpretation and FidelitY - MAGNIFY). Fundación CEAM is partly supported by Generalitat Valenciana, and the project DESESTRES (Prometeo Program - Generalitat Valenciana). EUPHORE instrumentation is partly funded by the Spanish Ministry of Science and Innovation, through INNPLANTA project: PCT-440000-2010-003. LV is indebted to the Max Planck Graduate Center with the Johannes Gutenberg-Universität Mainz (MPGC).

References

Ahrens, J., Carlsson, P. T. M., Hertl, N., Olzmann, M., Pfeifle, M., Wolf, J. L., and Zeuch, T.: Infrared Detection of Criegee Intermediates Formed during the Ozonolysis of β-pinene and Their Reactivity towards Sulfur Dioxide, Angew. Chem. Int. Ed. Engl., **53**, 715–719, 2014.

Alam, M. S., Camredon, M., Rickard, A. R., Carr, T., Wyche, K. P., Hornsby, K. E., Monks, P. S., and Bloss, W. J.: Total radical yields from tropospheric ethene ozonolysis, Phys. Chem. Chem. Phys., 13, 11002–11015, 2011.

Alam, M. S., Rickard, A. R., Camredon, M., Wyche, K. P., Carr, T., Hornsby, K. E., Monks, P. S., and Bloss, W. J.: Radical Product Yields from the Ozonolysis of Short Chain Alkenes under Atmospheric Boundary Layer Conditions, J. Phys. Chem. A, 117, 12468-12483, 2013.

Anglada, J. M., Gonzalez, J., and Torrent-Sucarrat, M.: Effects of the substituents on the reactivity of carbonyl oxides. A theoretical study on the reaction of substituted carbonyl oxides with water, Phys. Chem. Chem. Phys., 13, 13034–13045, 2011.

Anglada, M. and Sole, A.: Impact of the water dimer on the atmospheric reactivity of carbonyl oxides, Phys. Chem. Chem. Phys., 18, 17698-17712, 2016.

Asatryan, R. and Bozzelli, J.W.: Formation of a Criegee intermediate in the low-temperature oxidation of dimethyl sulfoxide, Phys. Chem. Chem. Phys., 10, 1769–1780, 2008.

Baptista, L., Pfeifer, L., da Silva, E. C., and Arbilla, G.: Kinetics and Thermodynamics of Limonene Ozonolysis, J. Phys. Chem. A, 115, 10911-10919, 2011.

Beck, M., Winterhalter, R., Herrmann, F., and Moortgat, G. K.: The gas-phase ozonolysis of α-humulene, Phys. Chem. Chem. Phys., 13, 10970–11001, 2011.

Becker, K. H.: EUPHORE: Final Report to the European Commission, Contract EV5V-CT92-0059, Bergische Universität Wuppertal, Germany, 1996.

Berndt, T., Voigtländer, J., Stratmann, F., Junninen, H., Mauldin III, R. L., Sipilä, M., Kulmala, M., and Herrmann, H.: Competing atmospheric reactions of CH_2OO with SO_2 and water vapour, Phys. Chem. Chem. Phys., 16, 19130–19136, 2014.

Berndt, T., Kaethner, R., Voigtländer, J., Stratmann, F., Pfiefle, M., Reichle, P., Sipilä, M., Kulmala, M., and Olzmann, M.: Kinetics of the unimolecular reaction of CH_2OO and the

bimolecular reactions with the water monomer, acetaldehyde and acetone at atmospheric conditions, Phys. Chem. Chem. Phys., 17, 19862–19873, 2015.

Berndt, T., Herrmann, H. and Kurtén, T.: Direct probing of Criegee intermediates from gas-phase ozonolysis using chemical ionization mass spectrometry, J. Am. Chem. Soc., DOI: 10.1021/jacs.7b05849, 2017.

Berresheim, H., Adam, M., Monahan, C., O'Dowd, C., Plane, J. M. C., Bohn, B., and Rohrer F.: Missing SO_2 oxidant in the coastal atmosphere? – observations from high-resolution measurements of OH and atmospheric sulfur compounds, Atmos. Chem. Phys., 14, 12209-12223, 2014.

Bey, I., Jacob, D. J., Yantosca, R. M., Logan, J. A., Field, B. D., Fiore, A. M., Li, Q., Liu, H. Y., Mickley, L. J., and Schultz, M. G.: Global modelling of tropospheric chemistry with assimilated meteorology: Model description and evaluation, J. Geophys. Res., 106, 23073–23095, 2001.

Blitz, M. A., Salter, R. J., Heard, D. E., and Seakins, P. J.: An Experimental and Master Equation Study of the Kinetics of OH/OD + SO_2: The Limiting High-Pressure Rate Coefficients, J. Phys. Chem. A, 121, 3184-3191, 2017.

Burkholder, J. B., Sander, S. P., Abbatt, J., Barker, J. R., Huie, R. E., Kolb, C. E., Kurylo, M. J., Orkin, V. L., Wilmouth, D. M., and Wine, P. H.: Chemical Kinetics and Photochemical Data for Use in Atmospheric Studies, Evaluation No. 18, JPL Publication 15-10, Jet Propulsion Laboratory, Pasadena, 2015 http://jpldataeval.jpl.nasa.gov.

Caravan, R. L., Khan, A. H. M., Rotavera, B., Papajak, E., Antonov, I. O., Chen, M. -W., Au, K., Chao, W., Osborn, D. L., Lin, J. J. -M., Percival, C. J., Shallcross, D. E., and Taatjes, C. E.: Products of Criegee intermediate reactions with NO_2: experimental measurements and tropospheric implications, Faraday Discuss., 200, 313-330, 2017.

Chang, Y.-P., Chang, H.-H. and Lin, J. J.-M.: Kinetics of the simplest Criegee intermediate reaction with ozone studied using a mid-infrared quantum cascade laser spectrometer, Phys. Chem. Chem. Phys., 20, 97–102, doi:10.1039/c7cp06653h, 2018.

Chao, W., Hsieh, J. -T., Chang, C. -H., and Lin, J. J. -M.: Direct kinetic measurement of the reaction of the simplest Criegee intermediate with water vapour, Science, DOI: 10.1126/science.1261549, 2015.

Chen, L., Wang, W., Wang, W., Liu, Y., Liu, F., Liu, N., and Wang, B.: Water-catalyzed decomposition of the simplest Criegee intermediate CH_2OO, Theor. Chem. Acc., 135:131, DOI 10.1007/s00214-016-1894-9, 2016.

Chhantyal-Pun, R., Davey, A., Shallcross, D. E., Percival, C. J., and Orr-Ewing, A. J.: A kinetic study of the CH_2OO Criegee intermediate self-reaction, reaction with SO_2 and unimolecular reaction using cavity ring-down spectroscopy, Phys. Chem. Chem. Phys., 17, 3617-3626, 2015.

Chhantyal-Pun, R., Welz, O., Savee, J. D., Eskola, A. J., Lee, E. P. F., Blacker, L., Hill, H. R., Ashcroft, M., Khan, M. A. H. H., Lloyd-Jones, G. C., Evans, L. A., Rotavera, B., Huang, H., Osborn, D. L., Mok, D. K. W., Dyke, J. M., Shallcross, D. E., Percival, C. J., Orr-Ewing, A. J. and Taatjes, C. A.: Direct Measurements of Unimolecular and Bimolecular Reaction Kinetics of the Criegee Intermediate $(CH_3)_2COO$, J. Phys. Chem. A, 121, 4-15, 2017

Chuong, B., Zhang, J, and Donahue, N. M.: Cycloalkene Ozonolysis: Collisionally Mediated Mechanistic Branching, J. Am. Chem. Soc., 126, 12363-12373, 2004.

Cox, R. A., and Penkett, S. A.: Oxidation of atmospheric SO_2 by products of the ozone-olefin reaction, Nature, 230, 321-322, 1971.

Crounse, J. D., Paulot, F., Kjaergaard, H. G., and Wennberg, P. O.: Peroxy radical isomerization in the oxidation of isoprene, Phys. Chem. Chem. Phys., 13, 13607-13613, 2011.

Crounse, J. D., Knap, H. C., Ørnsø, K. B., Jørgensen, S. Paulot, F., Kjaergaard, H. G., and Wennberg, P. O.: Atmospheric fate of methacrolein. 1. Peroxy radical isomerization following addition of OH and O_2, J. Phys. Chem. A., 116, 5756-5762, 2012.

Decker, Z. C. J., Au, K., Vereecken, L., and Sheps, L.: Direct experimental probing and theoretical analysis of the reaction between the simplest Criegee intermediate and CH_2OO and isoprene, Phys. Chem. Chem. Phys., 19, 8541-8551, 2017.

Donahue, N. M., Drozd, G. T., Epstein, S. A., Presto, A. A., and Kroll, J. H.: Adventures in ozoneland: down the rabbit-hole, Phys. Chem. Chem. Phys., 13, 10848-10857, 2011.

Drozd, G. T., and Donahue, N. M.: Pressure Dependence of Stabilized Criegee Intermediate Formation from a Sequence of Alkenes, J. Phys. Chem. A, 115, 4381-4387, 2011.

Eckart, C.: The penetration of a potential barrier by electrons, Phys. Rev., 35, 1303-1309, 1930.

Ehn, M., Thornton, J. A., Kleist, E., Sipilä, M., Junninen, H., Pulli- nen, I., Springer, M., Rubach, F., Tillmann, R., Lee, B., Lopez- Hilfiker, F., Andres, S., Acir, I.-H., Rissanen, M., Jokinen, T., Schobesberger, S., Kangasluoma, J., Kontkanen, J., Nieminen, T., Kurtén, T., Nielsen, L. B., Jørgensen, S., Kjaergaard, H. G., Canagaratna, M., Maso, M. D., Berndt, T., Petäjä, T., Wahner, A., Kerminen, V.-M., Kulmala, M., Worsnop, D. R., Wildt, J., and Mentel, T. F.: A large source of low-volatility secondary or- ganic aerosol., Nature, 506, 476–479, doi:10.1038/nature13032, 2014.

Fang, Y., Liu, F., Barber, V. P., Klippenstein, S. J., McCoy, A. B. and Lester, M. I.: Communication: Real time observation of unimolecular decay of Criegee intermediates to OH radical products, J. Chem. Phys., 144, 2016a.

Fang, Y., Liu, F., Klippenstein, S. J. and Lester, M. I.: Direct observation of unimolecular decay of CH3CH2CHOO Criegee intermediates to OH radical products, J. Chem. Phys., 145, 2016b.

Fenske, J. D., Hasson, A. S., Ho, A. W., and Paulson, S. E.: Measurement of absolute unimolecular and bimolecular rate constants for CH_3CHOO generated by the trans-2-butene reaction with ozone in the gas phase, J. Phys. Chem. A, 104, 9921–9932, 2000.

Foreman, E. S., Kapnas, K. M., and Murray, C.: Reactions between Criegee Intermediates and the Inorganic Acids HCl and HNO3: Kinetics and Atmospheric Implications, Angew. Chem. Int. Ed., 55, 1 – 5, 2016.

Frisch, M. J., Trucks, G. W., Schlegel, H. B., Scuseria, G. E., Robb, M. A., Cheeseman, J. R., Scalmani, G., Barone, V., Mennucci, B., Petersson, G. A., Nakatsuji, H., Caricato, M., Li, X., Hratchian, H. P., Izmaylov, A. F., Bloino, J., Zheng, G., Sonnenberg, J. L., Hada, M., Ehara, M., Toyota, K., Fukuda, R., Hasegawa, J., Ishida, M., Nakajima, T., Honda, Y., Kitao, O., Nakai, H., Vreven, T., Montgomery Jr., J. A., Peralta, J. E., Ogliaro, F., Bearpark, M., Heyd, J. J., Brothers, E., Kudin, K. N., Staroverov, V. N., Keith, T., Kobayashi, R., Normand, J., Normand, J., Raghavachari, K., Rendell, A., Burant, J. C., Iyengar, S. S., Tomasi, J., Cossi, M., Rega, N., Millam, J. M., Klene, M., Knox, J. E., Cross, J. B., Bakken, V., Adamo, C., Jaramillo, J., Gomperts, R., Stratmann, R. E., Yazyev, O., Austin, A. J., Cammi, R., Pomelli, C., Ochterski, J. W., Martin, R. L., Morokuma, K., Zakrzewski, V. G., Voth, G. A., Salvador, P., Dannenberg, J. J., Dapprich, S., Daniels, A. D., Farkas, O., Foresman, J. B., Ortiz, J. V.,

Cioslowski, J., Fox, D. J. and Pople, J. A.: Gaussian 09, Revision B.01, Gaussian Inc., Wallington CT., 2010.

Gravestock, T. J., Blitz, M. A., Bloss, W. J., and Heard, D. E.: A multidimensional study of the reaction CH_2I+O_2: Products and atmospheric implications, ChemPhysChem, 11, 3928 – 3941, 2010.

Guenther, A., Karl, T., Harley, P., Wiedinmyer, C., Palmer, P. I., and Geron, C.: Estimates of global terrestrial isoprene emissions using MEGAN (Model of Emissions of Gases and Aerosols from Nature), Atmos. Chem. Phys., 6, 3181-3210, 2006.

Guenther, A. B., Jiang, X., Heald, C. L., Sakulyanontvittaya, T., Duhl, T., Emmons, L. K., and Wang, X.: The Model of Emissions of Gases and Aerosols from Nature version 2.1 (MEGAN2.1): an extended and updated framework for modeling biogenic emissions, Geosci. Model Dev., 5, 1471-1492, 2012.

Gutbrod, R., Schindler, R. N., Kraka, E, and Cremer, D.: Formation of OH radicals in the gas phase ozonolysis of alkenes: the unexpected role of carbonyl oxides, Chem. Phys. Lett., 252, 221–229, 1996.

Hackenberg S. C., Andrews, S. J., Airs, R. L., Arnold, S. R., Bouman, H. A., Cummings, D., Lewis, A. C., Minaeian, J. K., Reifel, K. M., Small, A., Tarran, G. A., Tilstone, G. H., and Carpenter, L. J.: Basin-Scale Observations of Monoterpenes in the Arctic and Atlantic Oceans, Environ. Sci. Technol., 51, 10449−10458, 2017.

Hasson, A. S., Ho, A. W., Kuwata, K. T., and Paulson, S. E.: Production of stabilized Criegee intermediates and peroxides in the gas phase ozonolysis of alkenes 2. Asymmetric and biogenic alkenes, J. Geophys. Res., 106, 34143–34153, 2001.

Hatakeyama, S., Kobayashi, H., and Akimoto, H.: Gas-Phase Oxidation of SO_2 in the Ozone-Olefin Reactions, J. Phys. Chem., 88, 4736-4739, 1984.

Huang, H. -L., Chao, W., and Lin, J. J. -M.: Kinetics of a Criegee intermediate that would survive at high humidity and may oxidize atmospheric SO_2, Proc. Natl. Acad. Sci., 112, 10857–10862, 2015.

IUPAC Task Group on Atmospheric Chemical Kinetic Data Evaluation – Data Sheet Ox_VOC20, (http://iupac.pole-ether.fr), 2013.

IUPAC Task Group on Atmospheric Chemical Kinetic Data Evaluation – Data Sheet CGI_14_$(CH_3)_2COO$ + M, (http://iupac.pole-ether.fr), 2017.

Jalan, A., Allen, J. W., and Green, W. H.: Chemically activated formation of organic acids in reactions of the Criegee intermediate with aldehydes and ketones, Phys. Chem. Chem. Phys., 15, 16841-16852, 2013.

Jenkin, M. E., Saunders, S. M., and Pilling, M. J.: The tropospheric degradation of volatile organic compounds: a protocol for mechanism development, Atmos. Environ., 31, 81–104, 1997.

Jenkin, M. E., Young, J. C., and Rickard, A. R.: The MCM v3.3.1 degradation scheme for isoprene, Atmos. Chem. Phys., 15, 11433-11459, 2015.

Jiang, L., Lan, R., Xu, Y. -S., Zhang, W. -J., Yang, W.: Reaction of stabilized criegee intermediates from ozonolysis of limonene with water: Ab initio and DFT study, Int. J. Mol. Sci., 14, 5784-5805, 2013.

Johnson, D. and Marston, G.: The gas-phase ozonolysis of unsaturated volatile organic compounds in the troposphere, Chem. Soc. Rev., 37, 699–716, 2008.

Johnston, H. S. and Heicklen, J.: Tunneling corrections for unsymmetrical Eckart potential energy barriers, J. Phys. Chem., 66, 532–533, 1962.

Kidwell, N. M., Li, H., Wang, X., Bowman, J. M., and Lester, M. I.: Unimolecular dissociation dynamics of vibrationally activated CH_3CHOO Criegee intermediates to OH radical products, Nature Chemistry, 8, 509-514, 2016.

Kirkby, J., et al.: Ion-induced nucleation of pure biogenic particles, Nature, 533, 521-526, 2016.

Kjaergaard, H. G., Kurtén, T., Nielsen, L. B., Jørgensen, S., and Wennberg, P. O.: Criegee Intermediates React with Ozone, J. Phys. Chem. Lett., 4, 2525-2529, 2013.

Kotzias, D., Fytianos, K., and Geiss, F.: Reactions of monoterpenes with ozone, sulphur dioxide and nitrogen dioxide – Gas phase oxidation of SO_2 and formation of sulphuric acid, Atmos. Environ., 24, 2127-2132, 1990.

Kroll, J., Donahue, N. M., Cee, V. J., Demerjian, K. L., and Anderson, J. G.: Gas-phase ozonolysis of alkenes: formation of OH from anti carbonyl oxides, J. Am. Chem. Soc., 124, 8518–8519, 2002.

Kuwata, K. T., Guinn, E., Hermes, M. R., Fernandez, J., Mathison, J. and Huang, K.: A Computational Re-Examination of the Criegee Intermediate-Sulfur Dioxide Reaction, J. Phys. Chem. A, 119, 10316-10335, 2015.

Kuwata, K. T., Hermes, M. R., Carlson, M. J., and Zogg, C. K.: Computational Studies of the Isomerization and Hydration Reactions of Acetaldehyde Oxide and Methyl Vinyl Carbonyl Oxide, J. Phys Chem. A, 114, 9192-9204, 2010.

Lelieveld, J., Butler, T. M., Crowley, J. N., Dillon, T. J., Fischer, H., Ganzeveld, L., Harder, H., Lawrence, M. G., Martinez, M., Taraborrelli, D., and Williams, J.: Atmospheric oxidation capacity sustained by a tropical forest, Nature, 452, 737-740, 2008.

Leungsakul, S., Jaoui, M., and Kamens, R. M.: Kinetic Mechanism for Predicting Secondary Organic Aerosol Formation from the Reaction of *d*-limonene with Ozone, Environ. Sci. Technol., 39, 9583-9594, 2005.

Lewis, T. R., Blitz, M. A., Heard, D. E., and Seakins, P. W.: Direct evidence for a substantive reaction between the Criegee intermediate, CH_2OO, and the water vapour dimer, Phys. Chem. Chem. Phys., 17, 4859-4863, 2015.

Lin, L., Chang, H., Chang, C., Chao, W., Smith, M. C., Chang, C., Lin, J. J., and Takahashi, K.: Competition between H_2O and $(H_2O)_2$ reactions with CH_2OO/CH_3CHOO, Phys. Chem. Chem. Phys., 18, 4557-4568, 2016a.

Lin, L. -C., Chao, W., Chang, C. -H., Takahashi, K., and Lin, J. J. -M.: Temperature dependence of the reaction of: Anti-CH_3CHOO with water vapor, Phys. Chem. Chem. Phys., 18, 28189-28197, 2016b.

Liu, Y., Liu, F., Liu, S., Dai, D., Dong, W., and Yang, X.: A kinetic study of the CH_2OO Criegee intermediate reaction with SO_2, $(H_2O)_2$, CH_2I_2 and I atoms using OH laser induced fluorescence, Phys. Chem. Chem. Phys., 19, 20786-20794, 2017.

Long, B., Bao, J. L. and Truhlar, D. G.: Atmospheric Chemistry of Criegee Intermediates. Unimolecular Reactions and Reactions with Water, J. Am. Chem. Soc., 138, 14409-14422, 2016.

Luo, G., and Yu, F.: A numerical evaluation of global oceanic emissions of α-pinene and isoprene, Atmos. Chem. Phys., 10, 2007–2015, 2010.

Ma, Y., Russell, A. T., and Marston, G.: Mechanisms for the formation of secondary organic aerosol components from the gas-phase ozonolysis of α-pinene, Phys. Chem. Chem. Phys., 10, 4294-4312, 2008.

Ma, Y., and Marston, G.: Multi-functional acid formation from the gas-phase ozonolysis of β-pinene, Phys. Chem. Chem. Phys., 10, 6115-6126, 2008.

Mao, J., Jacob, D. J., Evans, M. J., Olson, J. R., Ren, X., Brune, W. H., St. Clair, J. M., Crounse, J. D., Spencer, Beaver, M. R., Wennberg, P. O., Cubison, M. J., Jimenez, J. L., Fried, A., Weibring, P., Walega, J. G., Hall, S. R., Weinheimer, A. J., Cohen, R. C., Chen, G., Crawford, J. H., Jaeglé, L., Fisher, J. A., Yantosca, R. M., Le Sager, P., and Carouge, C.: Chemistry of hydrogen oxide radicals (HOx) in the Arctic troposphere in spring, Atmos. Chem. Phys., 10, 5823-5838, 2010.

Mao, J., Paulot, F., Jacob, D. J., Cohen, R. C., Crounse, J. D., Wennberg, P. O., Keller, C. A., Hudman, R. C., Barkley, M. P., and Horowitz, L. W.: Ozone and organic nitrates over the eastern United States: Sensitivity to isoprene chemistry, J. Geophys. Res., 118, 11256–11268, 2013.

Martinez, R. I., and Herron, J. T.: Stopped-flow studies of the mechanisms of alkene-ozone reactions in the gas-phase: tetramethylethylene, J. Phys. Chem., 91, 946-953, 1987.

Mauldin III, R. L., Berndt, T., Sipilä, M., Paasonen, P., Petäjä, T., Kim, S., Kurtén, T., Stratmann, F., Kerminen, V.-M., and Kulmala, M.: A new atmospherically relevant oxidant, Nature, 488, 193–196, 2012.

Newland, M. J., Rickard, A. R., Alam, M. S., Vereecken, L., Muñoz, A., Ródenas, M., and Bloss, W. J.: Kinetics of stabilised Criegee intermediates derived from alkene ozonolysis: reactions with SO_2, H_2O and decomposition under boundary layer conditions, Phys. Chem. Chem. Phys., 17, 4076, 2015a.

Newland, M. J., Rickard, A. R., Vereecken, L., Muñoz, A., Ródenas, M., and Bloss, W. J.: Atmospheric isoprene ozonolysis: impacts of stabilised Criegee intermediate reactions with SO_2, H_2O and dimethyl sulfide, Atmos. Chem. Phys., 15, 9521–9536, 2015b.

Nguyen, T. L., Peeters, J., and Vereecken, L.: Theoretical study of the gas-phase ozonolysis of β-pinene ($C_{10}H_{16}$), Phys. Chem. Chem. Phys., 11, 5643–5656, 2009a.

Nguyen, T. L., Winterhalter, R., Moortgat, G., Kanawati, B., Peeters, J., and Vereecken, L.: The gas-phase ozonolysis of β-caryophyllene ($C_{15}H_{24}$). Part II: A theoretical study, Phys. Chem. Chem. Phys., 11, 4173–4183, 2009b.

Nguyen, T. L., Lee, H., Matthews, D. A., McCarthy, M. C. and Stanton, J. F.: Stabilization of the Simplest Criegee Intermediate from the Reaction between Ozone and Ethylene: A High Level Quantum Chemical and Kinetic Analysis of Ozonolysis, J. Phys. Chem. A, 119, 5524-5533, 2015.

Niki, H., Maker, P. D., Savage, C. M., Breitenbach, L. P., and Hurley, M. D.: FTIR spectroscopic study of the mechanism for the gas-phase reaction between ozone and tetramethylethylene, J. Phys. Chem., 91, 941–946, 1987.

Novelli, A., Vereecken, L., Lelieveld, J., and Harder, H.: Direct observation of OH formation from stabilised Criegee intermediates, Phys. Chem. Chem. Phys., 16, 19941–19951, 2014.

Parrella, J. P., Jacob, D. J., Liang, Q., Zhang, Y., Mickley, L. J., Miller, B., Evans, M. J., Yang, X., Pyle, J. A., Theys, N., and Van Roozendael, M.: Tropospheric bromine chemistry: implications for present and pre-industrial ozone and mercury, Atmos. Chem. Phys., 12, 6723-6740, 2012.

Paulot, F., Crounse, J. D., Kjaergaard, H. G., Kürten, A., Clair, J. M. S., Seinfeld, J. H., and Wennberg, P. O.: Unexpected epoxide formation in the gas-phase photooxidation of isoprene, Science, 325, 730-733, 2009a.

Paulot, F., Crounse, J. D., Kjaergaard, H. G., Kroll, J. H., Seinfeld, J. H., and Wennberg, P. O.: Isoprene photooxidation: New insights into the production of acids and organic nitrates, Atmos. Chem. Phys., 9, 1479-1501, 2009b.

Paulson, S. E., Chung, M., Sen, A. D., and Orzechowska, G.: Measurement of OH radical formation from the reaction of ozone with several biogenic alkenes, Geophys. Res. Lett., 24, 3193–3196, 1997.

Peeters, J., Nguyen, T. L., and Vereecken, L.: HOx radical regeneration in the oxidation of isoprene, Phys. Chem. Chem. Phys., 11, 5935-5939, 2009.

Peeters, J., and Müller, J. F.: HOx radical regeneration in isoprene oxidation via peroxy radical isomerisations. II: Experimental evidence and global impact, Phys. Chem. Chem. Phys., 12, 14227-14235, 2010.

Pöschl, U., and Shiraiwa, M.: Multiphase Chemistry at the Atmosphere-Biosphere Interface Influencing Climate and Public Health in the Anthropocene, Chem. Rev., 115, 4440–4475, 2015.

Rickard, A. R., Johnson, D., McGill, C. D., and Marston, G.: OH Yields in the Gas-Phase reactions of Ozone with Alkenes, J. Phys. Chem. A, 103, 7656–7664, 1999.

Rossignol, S., Rio, C., Ustache, A., Fable, S., Nicolle, J., Même, A., D'Anna, B., Nicolas, M., Leoz, E., and Chiappini, L.: The use of a housecleaning product in an indoor environment leading to oxygenated polar compounds and SOA formation: Gas and particulate phase chemical characterization, Atmos. Environ., 75, 196-205, 2013.

Ryzhkov, A. B., and P. A. Ariya, A theoretical study of the reactions of parent and substituted Criegee intermediates with water and the water dimer, Phys. Chem. Chem. Phys., 6, 5042-5050, 2004.

Sarwar, G., and Corsi, R.: The effects of ozone/limonene reactions on indoor secondary organic aerosols, Atmos. Environ., 41, 959–973, 2007.

Saunders, S. M., Jenkin, M. E., Derwent, R. G., and Pilling, M. J.: Protocol for the development of the Master Chemical Mechanism, MCM v3 (Part A): Tropospheric degradation of non-aromatic volatile organic compounds, Atmos. Chem. Phys., 3, 161-180, 2003.

Shallcross, D. E., Taatjes, C. A., and Percival, C. J.: Criegee intermediates in the indoor environment: new insights, Indoor Air, 24, 495–502, 2014.

Sheps, L., Scully, A. M., and Au, K.: UV absorption probing of the conformer-dependent reactivity of a Criegee intermediate CH_3CHOO Phys. Chem. Chem. Phys., 16, 26701-26706, 2014.

Sheps, L., Rotavera, B., Eskola, A. J., Osborn, D. L., Taatjes, C. A., Au, K., Shallcross, D. E., Khan, M. A. H., and Percival, C. J.: The reaction of Criegee intermediate CH_2OO with water dimer: primary products and atmospheric impact, Phys. Chem. Chem. Phys., 19, 21970–21979, 2017.

Sindelarova, K., Granier, C., Bouarar, I., Guenther, A., Tilmes, S., Stavrakou, T., Müller, J.-F., Kuhn, U., Stefani, P., and Knorr, W.: Global data set of biogenic VOC emissions

calculated by the MEGAN model over the last 30 years, Atmos. Chem. Phys., 14, 9317-9341, 2014.

Singer, B. C., Coleman, B. K., Destaillats, H., Hodgson, A. T., Lunden, M. M., Weschler, C. J., and Nazaroff, W. W.: Indoor secondary pollutants from cleaning product and air freshener use in the presence of ozone, Atmos. Environ., 40, 6696-6710, 2006a.

Singer, B. C., Destaillats, H., Hodgson, A. T., and Nazaroff, W. M.: Cleaning products and air fresheners: emissions and resulting concentrations of glycol ethers and terpenoids, Indoor Air, 16, 179-191, 2006b.

Sipilä, M., Jokinen, T., Berndt, T., Richters, S., Makkonen, R., Donahue, N. M., Mauldin III, R. L., Kurtén, T., Paasonen, P., Sarnela, N., Ehn, M., Junninen, H., Rissanen, M. P., Thornton, J., Stratmann, F., Herrmann, H., Worsnop, D. R., Kulmala, M., Kerminen, V.-M., and Petäjä, T.: Reactivity of stabilized Criegee intermediates (sCIs) from isoprene and monoterpene ozonolysis toward SO_2 and organic acids, Atmos. Chem. Phys., 14, 12143-12153, 2014.

Smith, M. C., Chao, W., Takahashi, K., Boering, K. A., and Lin, J. J. -M.: Unimolecular Decomposition Rate of the Criegee Intermediate $(CH_3)_2COO$ Measured Directly with UV Absorption Spectroscopy, J. Phys. Chem. A, doi: 10.1021/acs.jpca.5b12124, 2016.

Stone, D., Blitz, M., Daubney, L., Howes, N. U. M., and Seakins, P.: Kinetics of CH_2OO reactions with SO_2, NO_2, NO, H_2O, and CH_3CHO as a function of pressure, Phys. Chem. Chem. Phys., 16, 1139-1149, 2014.

Su, Y. -T., Lin, H. -Y., Putikam, R., Matsui, H., Lin, M. C., and Lee, Y. -P.: Extremely rapid self-reaction of the simplest Criegee intermediate CH_2OO and its implications in atmospheric chemistry, Nature Chemistry, 6, 477-483, 2014.

Taatjes, C. A., Welz, O., Eskola, A. J., Savee, J. D., Osborn, D. L., Lee, E. P. F., Dyke, J. M., Mok, D. W. K., Shallcross, D. E., and Percival, C. J.: Direct measurements of Criegee intermediate (CH_2OO) formed by reaction of CH_2I with O_2, Phys. Chem. Chem. Phys., 14, 10391-10400, 2012.

Taatjes, C. A., Welz, O., Eskola, A. J., Savee, J. D., Scheer, A. M., Shallcross, D. E., Rotavera, B., Lee, E. P. F., Dyke, J. M., Mok, D. K. W., Osborn, D. L., and Percival, C. J.: Direct Measurements of Conformer-Dependent Reactivity of the Criegee Intermediate CH_3CHOO, Science, 340, 177–180, 2013.

Taatjes, C. A., Shallcross, D. E., and Percival, C. J.: Research frontiers in the chemistry of Criegee intermediates and tropospheric ozonolysis, Phys. Chem. Chem. Phys., 16, 1704-1718, 2014.

Taipale, R., Sarnela, N., Rissanen, M., Junninen, H., Rantala, P., Korhonen, F., Siivola, E., Berndt, T., Kulmala, M., Mauldin, R.L. III, Petäjä, T., Sipilä, M.: New instrument for measuring atmospheric concentrations of non-OH oxidants of SO_2, Bor. Env. Res., 19 (suppl. B), 55-70, 2014.

Truhlar, D. G., Garrett, B. C. and Klippenstein, S. J.: Current Status of Transition-State Theory, J. Phys. Chem., 100, 12771-12800, 1996.

Vereecken, L. and Peeters, J.: The 1,5-H-shift in 1-butoxy: A case study in the rigorous implementation of transition state theory for a multirotamer system, J. Chem. Phys., 119, 5159-5170, 2003.

Vereecken, L., and Francisco, J. S.: Theoretical studies of atmospheric reaction mechanisms in the troposphere, Chem. Soc. Rev., 41, 6259-6293, 2012.

Vereecken, L., Harder, H., and Novelli, A.: The reaction of Criegee intermediates with NO, RO_2, and SO_2, and their fate in the atmosphere, Phys. Chem. Chem. Phys., 14, 14682–14695, 2012.

Vereecken, L., Harder, H., and Novelli, A.: The reactions of Criegee intermediates with alkenes, ozone and carbonyl oxides, Phys. Chem. Chem. Phys., 16, 4039–4049, 2014.

Vereecken, L., Rickard, A. R., Newland, M. J., and Bloss, W. J.: Theoretical study of the reactions of Criegee intermediates with ozone, alkylhydroperoxides, and carbon monoxide, Phys. Chem. Chem. Phys., 17, 23847–23858, 2015.

Vereecken, L., and Nguyen, H. M. T.: Theoretical Study of the Reaction of Carbonyl Oxide with Nitrogen Dioxide: $CH_2OO + NO_2$, Int. J. Chem. Kinet., 49, 752-760, 2017.

Vereecken, L.: The Reaction of Criegee Intermediates with Acids and Enols, Phys. Chem. Chem. Phys., DOI: 10.1039/C7CP05132H, 2017.

Vereecken, L., Novelli, A. and Taraborrelli, D.: Unimolecular decay strongly limits concentration of Criegee intermediates in the atmosphere, Phys. Chem. Chem. Phys., 19, 31599–31612, doi:10.1039/C7CP05541B, 2017.

Wang, L., and Wang, L.: Mechanism of gas-phase ozonolysis of sabinene in the atmosphere, Phys. Chem. Chem. Phys., doi: 10.1039/c7cp03216a, 2017.

Wei, W., Zheng, R., Pan, Y., Wu, Y., Yang, F., and Hong, S.: Ozone Dissociation to Oxygen Affected by Criegee Intermediate, J. Phys. Chem. A, 118, 1644–1650, 2014.

Wei, W. -M., Yang, X., Zheng, R. -H., Qin, Y. -D., Wu, Y. -K., Yang, F.: Theoretical studies on the reactions of the simplest Criegee intermediate CH_2OO with CH_3CHO, Comp. Theor. Chem., 1074, 142-149, 2015.

Welz, O., Eskola, A. J., Sheps, L., Rotavera, B., Savee, J. D., Scheer, A. M., Osborn, D. L., Lowe, D., Murray Booth, A., Xiao, P., Anwar H., Khan, M., Percival, C. J., Shallcross, D. E., and Taatjes, C. A.: Rate coefficients of C1 and C2 Criegee intermediate reactions with formic and acetic acid near the collision limit: direct kinetics measurements and atmospheric implications, Angew. Chem. Int. Ed. Engl., 53, 4547–4750, 2014.

Welz, O., Savee, J. D., Osborn, D. L., Vasu, S. S., Percival, C. J., Shallcross, D. E., and Taatjes, C. A.: Direct Kinetic Measurements of Criegee Intermediate (CH_2OO) Formed by Reaction of CH_2I with O_2, Science, 335, 204–207, 2012.

Winterhalter, R., Neeb, P., Grossmann, D., Kolloff, A., Horie, O., and Moortgat, G.: Products and Mechanism of the Gas Phase Reaction of Ozone with β-pinene, J. Atmos. Chem., 35, 165-197, 2000.

Yao, L., Ma, Y., Wang, L., Zheng, J., Khalizov, A., Chen, M., Zhou, Y., Qi, L., and Cui, F.: Role of stabilized Criegee Intermediate in secondary organic aerosol formation from the ozonolysis of α-cedrene, Atmos. Environ., 94, 448-457, 2014.

Zhang, D., and Zhang, R.: Ozonolysis of α-pinene and β-pinene: Kinetics and mechanism, J. Chem. Phys., 122, 114308, 2005.

Zhang, J., Huff Hartz, K. E., Pandis, S. N., and Donahue, N. M.: Secondary Organic Aerosol Formation from Limonene Ozonolysis: Homogeneous and Heterogeneous Influences as a Function of NO_x, J. Phys. Chem. A, 110, 11053-11063, 2006.

Zhou, L., Gierens, R., Sogachev, A., Mogensen, D., Ortega, J., Smith, J. N., Harley, P. C., Prenni, A. J., Levin, E. J. T., Turnipseed, A., Rusanen, A., Smolander, S., Guenther, A. B., Kulmala, M., Karl, T., and Boy, M.: Contribution from biogenic organic compounds to particle growth during the 2010 BEACHON-ROCS campaign in a Colorado temperate needle

leaf forest, Atmos. Chem. Phys. Discuss., 15, 9033-9075, doi:10.5194/acpd-15-9033-2015, 2015.

Table 1. Monoterpene SCI yields derived in this work and reported in the literature.

ϕ_{SCI}	Reference	Notes	Methodology
α-pinene			
0.19 (± 0.01)	This work		SO_2 loss
0.15 (± 0.07)	Sipilä et al. (2014)		Formation of H_2SO_4
0.22	Taipale et al. (2014) (personal comm. Berndt)		
0.125 (± 0.04)	Hatakeyama et al. (1984)		Formation of H_2SO_4
0.20	MCMv3.3.1 [a]		
β-pinene			
0.60 (± 0.03)	This work		SO_2 loss
0.46	Ahrens et al. (2014)	$\varphi_{C9\text{-}SCI:}$ 0.36 $\varphi_{CH2OO:}$ 0.10	FTIR detection
0.25	MCMv3.3.1 [a]	$\varphi_{C9\text{-}SCI:}$ 0.102 $\varphi_{CH2OO:}$ 0.148	
0.42	Nguyen et al. (2009)	$\varphi_{C9\text{-}SCI:}$ 0.37 $\varphi_{CH2OO:}$ 0.05	Theoretical
0.51	Winterhalter et al. (2000)	$\varphi_{C9\text{-}SCI:}$ 0.35 $\varphi_{CH2OO:}$ 0.16	Change in nopinone yields $f([H_2O])$
0.44	Kotzias et al. (1990)		Formation of H_2SO_4
0.25	Hatakeyama et al. (1984)		Formation of H_2SO_4
0.30	Zhang and Zhang (2005)	$\varphi_{C9\text{-}SCI:}$ 0.22 $\varphi_{CH2OO:}$ 0.08	
> 0.27	Ma and Marston (2008)	$\varphi_{C9\text{-}SCI:}$ 0.27 $\varphi_{CH2OO:}$ 0.16[a] $\varphi_{CH2OO:}$ 0.06[b]	Change in nopinone yields $f([H_2O])$
0.27	Hasson et al. (2001)		Change in nopinone yields $f([H_2O])$
Limonene			
0.23 (± 0.01)	This work		SO_2 loss
0.27 (± 0.12)	Sipilä et al. (2014)		Formation of H_2SO_4
0.34	Leungsakul et al. (2005)	$\varphi_{C10\text{-}SCI:}$ 0.26 $\varphi_{CI\text{-}x:}$ 0.04	Measurement of stable particle and

		$\varphi_{CH2OO:}$ 0.05	gas-phase products
0.135	MCMv3.3.1 [a]		

Uncertainty ranges (± 2σ, parentheses) indicate combined precision and systematic measurement error components for this work, and are given as stated for literature studies. All referenced experimental studies produced SCI from MT + O_3 and were conducted between 700 and 760 Torr. [a] http://mcm.leeds.ac.uk/MCM/ (Jenkin et al., 2015).

[a] assuming 100 % stabilisation
[b] assuming 40 % stabilisation

Table 2. Monoterpene derived SCI relative and absolute[a] rate constants derived in this work.

SCI	$10^5\ k_3/k_2$	$10^{15}\ k_3$ ($cm^3\ s^{-1}$)	$10^{-12}\ k_d/k_2$ (cm^{-3})	k_d (s^{-1})
α-pinene				
SCI-A	> 140 (± 34)	> 310 (± 75)[a]		
SCI-B			< 8.2 (± 1.5)	< 240 (± 44)[c]
β-pinene				
SCI-A	> 10 (± 2.7)	> 4 (± 1)[b]		
SCI-B			< 6.0 (± 1.3)	< 170 (± 38)[c]
Limonene				
SCI-A	< 3.5 (± 0.2)	< 7.7 (± 0.6)[a]		
SCI-B			> 4.5 (± 0.1)	> 130 (± 3)[c]

Uncertainty ranges (± 2σ, parentheses) indicate combined precision and systematic measurement error components. [a] Scaled to an absolute value using k_2(anti-CH_3CHOO) = 2.2×10^{-10} $cm^3\ s^{-1}$ (Sheps et al., 2014); [b] Scaled to an absolute value using k_2(anti-CH_3CHOO) = 4×10^{-11} $cm^3\ s^{-1}$ (Ahrens et al., 2014); [c] Scaled using k_2(*syn*-CH_3CHOO) = 2.9×10^{-11} $cm^3\ s^{-1}$ (Sheps et al., 2014).

Table 3. Unimolecular reactions for the CI derived from α-pinene, β-pinene, and *d*-limonene, as derived by Vereecken et al. (2017). Barrier heights (kcal mol^{-1}) listed estimate post-CCSD(T) energies.

Carbonyl oxide	**Reaction**	E_b	k**(298K) / s^{-1}**
α-pinene			
CI-1a	1,4-H-migration	15.8	600
	SOZ-formation	15.6	5×10^{-2}
	1,3-ring closure	21.6	1×10^{-3}
CI-1b	1,3-ring closure	14.8	60
	1,3-H-migration	29.0	1×10^{-6}
CI-2a	1,4-H-migration	16.3	250
	1,3-ring closure	20.8	6×10^{-3}
CI-2b	1,4-H-migration	17.0	60
	SOZ-formation	13.5	8
	Ring closure	19.9	3×10^{-2}
β-pinene			
CI-3	1,4-H-migration	15.7	375
	1,3-ring closure	21.1	2×10^{-3}
CI-4	1,3-ring closure	17.2	2.0
	Ring opening	23.6	(Slow, Nguyen et al. 2009a)
	1,4-H-migration	24.9	(Slow, Nguyen et al. 2009a)
CH_2OO	1,3-ring closure	19.0	0.3
	1,3-H-migration	30.7	1×10^{-7}
Limonene[a]			
CI-5a	1,4-H-migration	SAR	200 [a]
CI-5b	1,3-ring closure	SAR	75 [a]
CI-6a	1,4-H-migration	SAR	430 [a]
CI-6b	1,4-H-migration	SAR	700 [a]
CI-7a	1,4-H-migration	SAR	15
CI-7b	1,4-H-migration	SAR	600

[a] Formation of secondary ozonides (SOZ) is not included, and could be the dominant unimolecular loss.

Table 4. Rate coefficients (cm^3 $molecule^{-1}$ s^{-1}) for the reaction of CI with H_2O and $(H_2O)_2$ as predicted by Vereecken et al. (2017). Values are based on explicit CCSD(T)/aug-cc-pVTZ//M06-2X/aug-cc-pVTZ calculations and multi-conformer TST, including empirical corrections to reference experimental data, except for limonene-derived CI where the values are predicted using a structure-activity relationship. The rate coefficients for CH_2OO, CH_3CHOO, and $(CH_3)_2COO$ are within a factor of 4 of evaluated literature data (Vereecken et al., 2017).

Carbonyl oxide	***k*(298K) H_2O**	***k*(298K) $(H_2O)_2$**
CH_2OO	8.7×10^{-16}	1.4×10^{-12}
syn-CH_3CHOO	6.7×10^{-19}	2.1×10^{-15}
anti-CH_3CHOO	2.3×10^{-14}	2.7×10^{-11}
$(CH_3)_2COO$	7.5×10^{-18}	1.8×10^{-14}
α-pinene		
CI-1a	1.3×10^{-18}	2.9×10^{-15}
CI-1b	1.5×10^{-14}	1.7×10^{-11}
CI-2a	1.0×10^{-18}	2.5×10^{-15}
CI-2b	2.4×10^{-19}	7.0×10^{-16}
β-pinene		
CI-3	1.7×10^{-18}	4.3×10^{-15}
CI-4	4.2×10^{-16}	6.4×10^{-13}
Limonene		
CI-5a	1.5×10^{-18}	4.3×10^{-15}
CI-5b	1.5×10^{-14}	1.7×10^{-11}
CI-6a	9.1×10^{-18}	2.1×10^{-14}
CI-6b	1.5×10^{-17}	3.2×10^{-14}
CI-7a	9.7×10^{-18}	1.9×10^{-14}
CI-7b	4.3×10^{-18}	1.1×10^{-14}

Table 5. Kinetic parameters used in the global modelling study.

SCI	ϕ_{SCI}	$10^{15}\ k_3$ ($cm^3\ s^{-1}$)	$10^{11}\ k_2$ [a] ($cm^3\ s^{-1}$)	k_d (s^{-1})
α-pinene				
SCI-A	0.08	310	22	-
SCI-B	0.11	-	2.9	240
β-pinene				
SCI-A	0.25	4	4	-
SCI-B	0.35	-	2.9	170
Limonene				
SCI-A	0.05	7.7	22	-
SCI-B	0.18	-	2.9	130
Myrcene				
SCI-B	0.30	-	13[b]	400[c]
Ocimene				
SCI-B	0.30	-	13[b]	400[c]
Sabinene [d]				
SCI-A	0.25	4	4	-
SCI-B	0.35	-	2.9	170
3-carene [e]				
SCI-A	0.08	310	22	-
SCI-B	0.11	-	2.9	240

[a] k_2(SCI-A+SO_2) from (SO_2+*anti*-CH_3CHOO) - Sheps et al. (2014); k_2(SCI-B+SO_2) from (SO_2+*syn*-CH_3CHOO) - Sheps et al. (2014) unless otherwise stated

[b] k_2(SCI-B+SO_2) from (SO_2+*anti*-$(CH_3)_2COO$) – Huang et al. (2015)

[c] Temp dependent k_d(SCI-B) taken from IUPAC recommendation (2017)

[d] Kinetics based on β-pinene

[e] Kinetics based on α-pinene

Table 6. Monoterpene contribution to [SCI] and SO_2 oxidation in the surface layer of the model simulation.

Monoterpene	Annual emissions[a] (Tg C)	% contribution to [SCI-A]	% contribution to [SCI-B]	% contribution to SO_2 oxidation
α-pinene	35.4	0.5	15	5.8
β-pinene	16.9	74	43	54
limonene	9.2	3.5	13	6.0
myrcene	3.1	0.0	2.7	9.0
trans-β-ocimene	14.1	0.0	11	20
sabinene	7.9	22	13	3.8
3-carene	6.4	0.0	2.5	1.3

[a] From MEGAN v2.1 (Guenther et al., 2012)

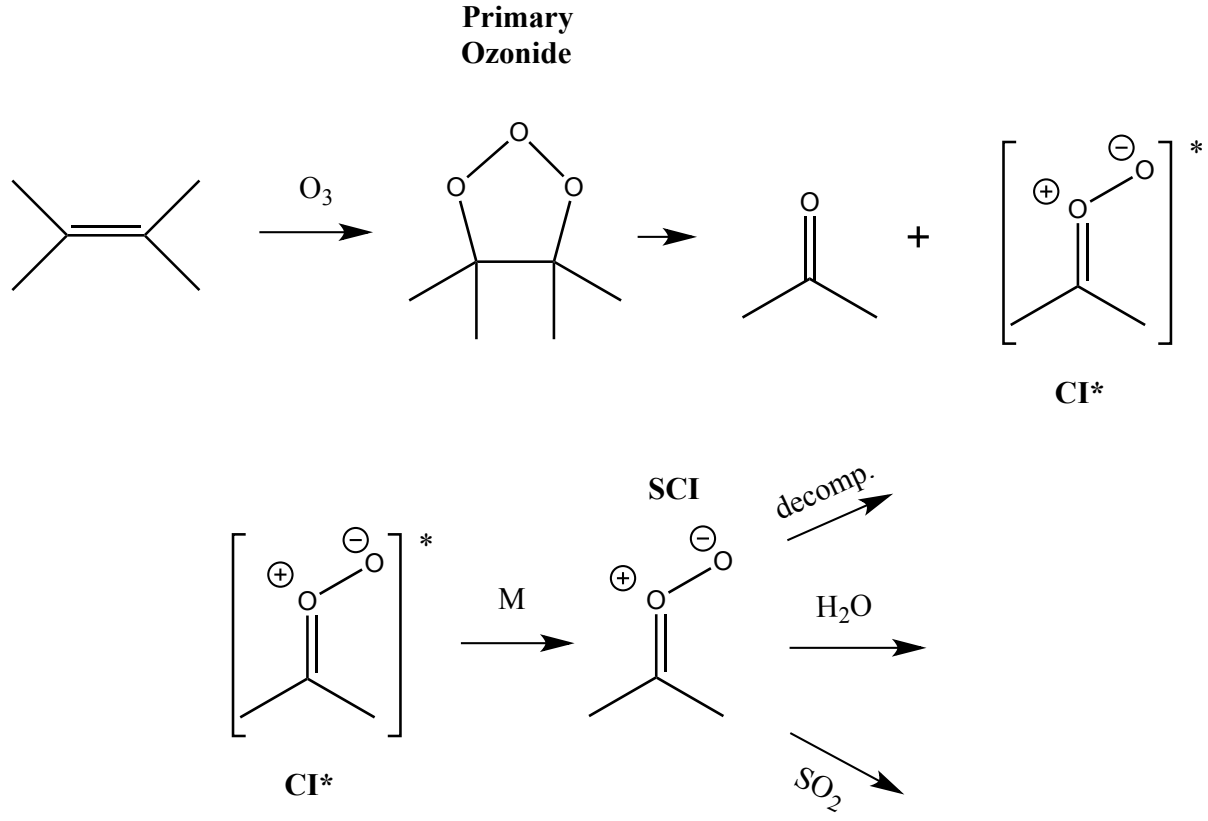

Scheme 1. Simplified generic mechanism for the reaction of Criegee Intermediates (CIs) formed from alkene ozonolysis.

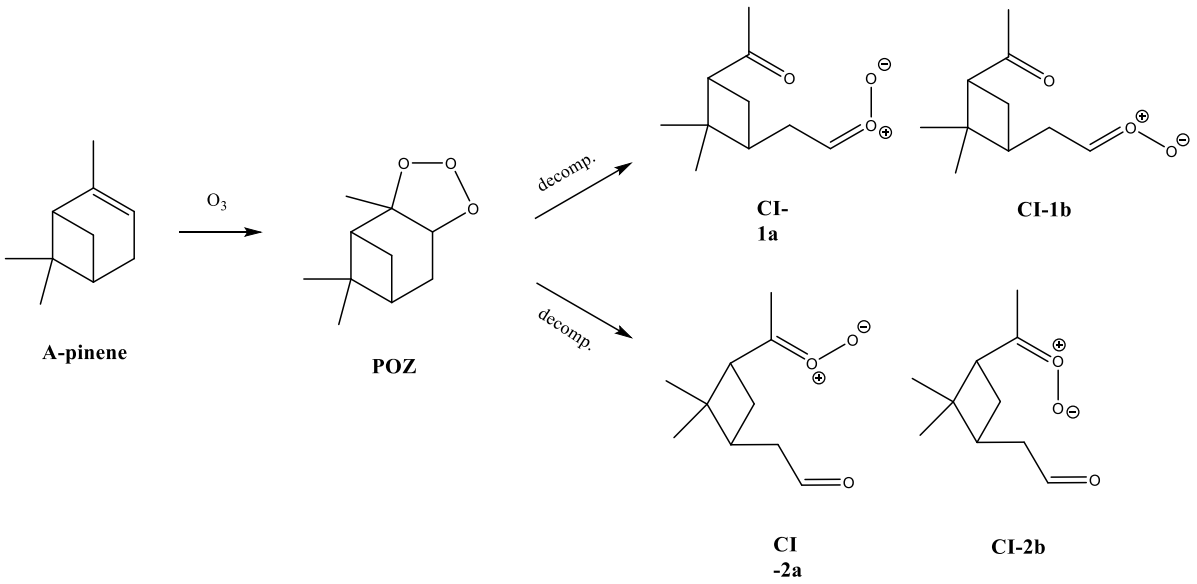

Scheme 2. Mechanism of formation of the two Criegee Intermediates (CIs) from α-pinene ozonolysis.

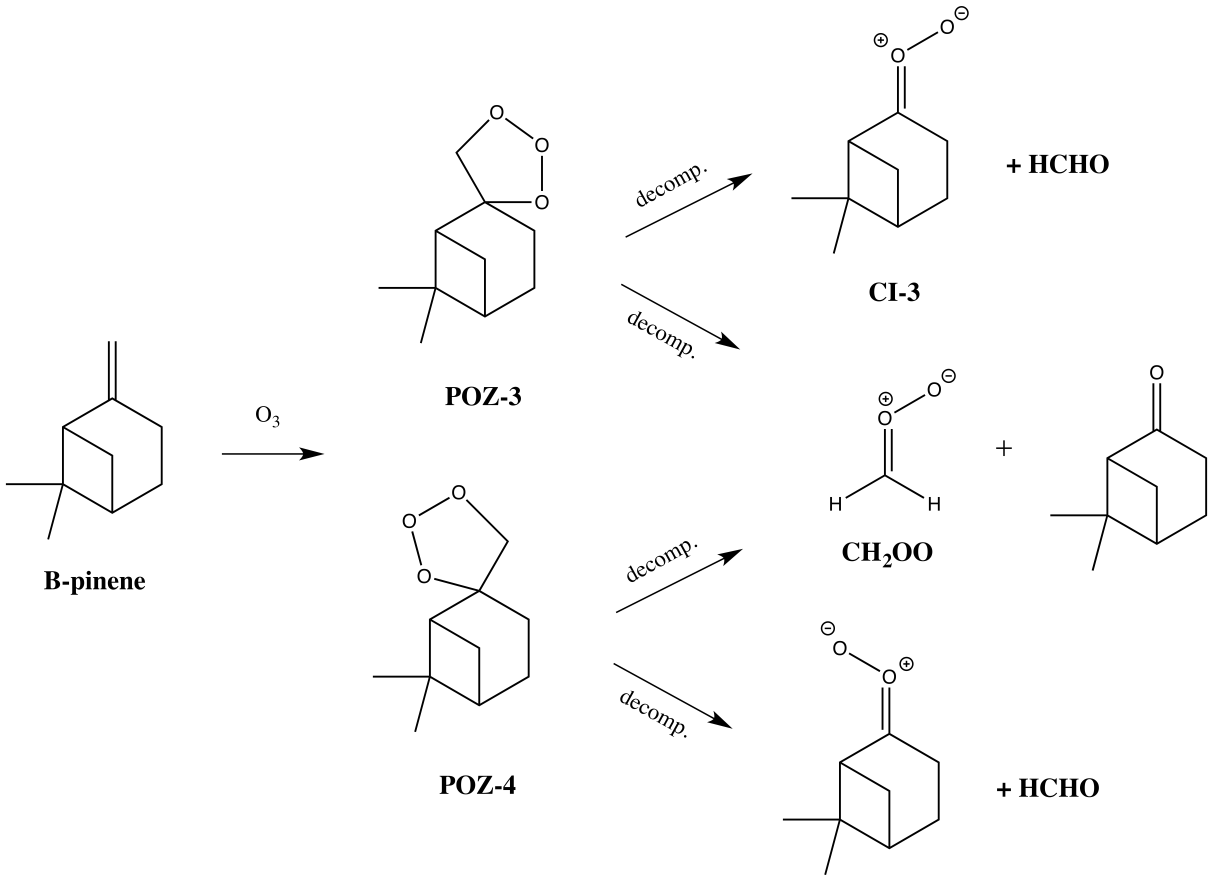

Scheme 3. Mechanism of formation of the three Criegee Intermediates (CIs) from β-pinene ozonolysis.

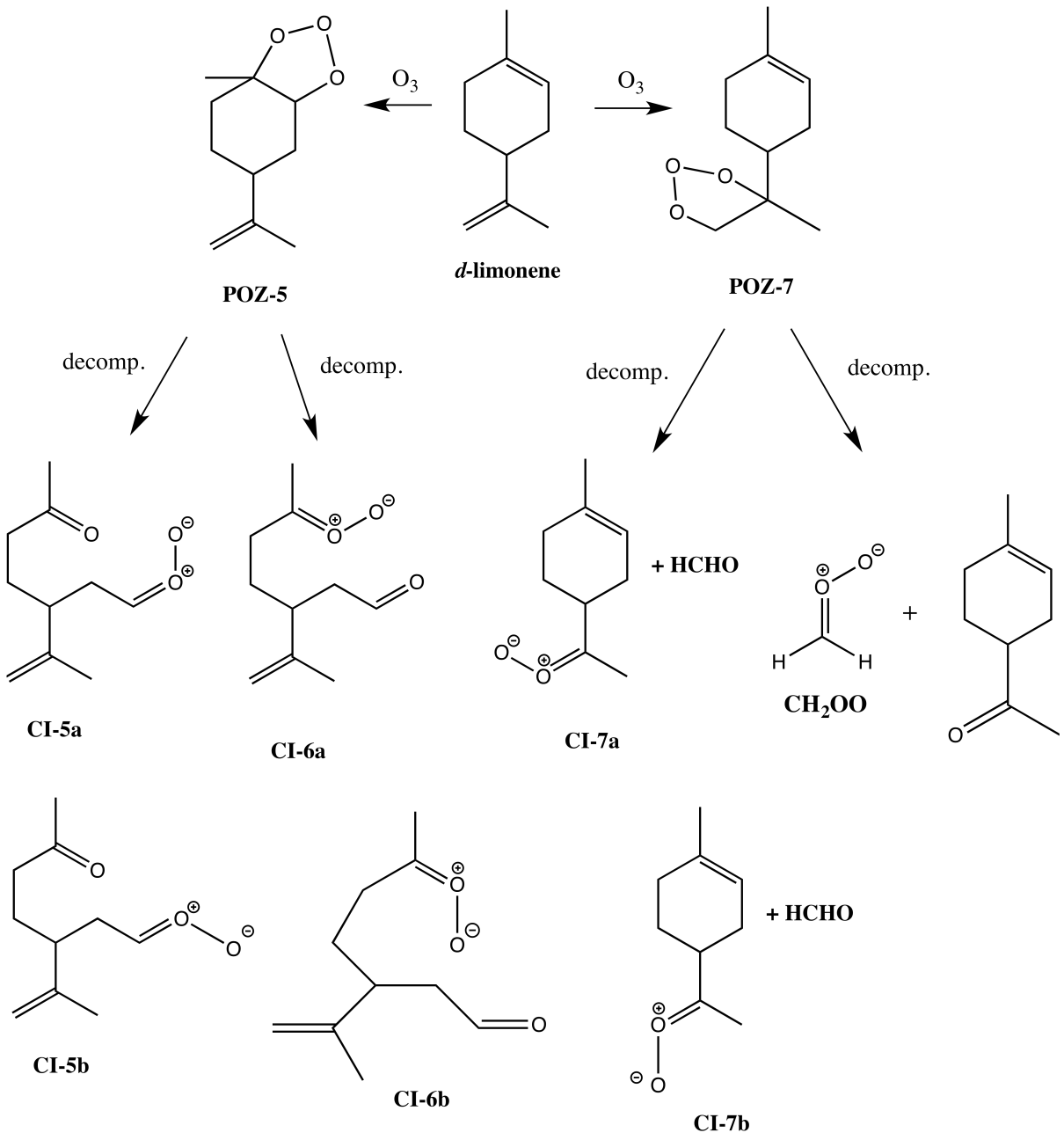

Scheme 4. Mechanism of formation of the four Criegee Intermediates (CIs) from limonene ozonolysis.

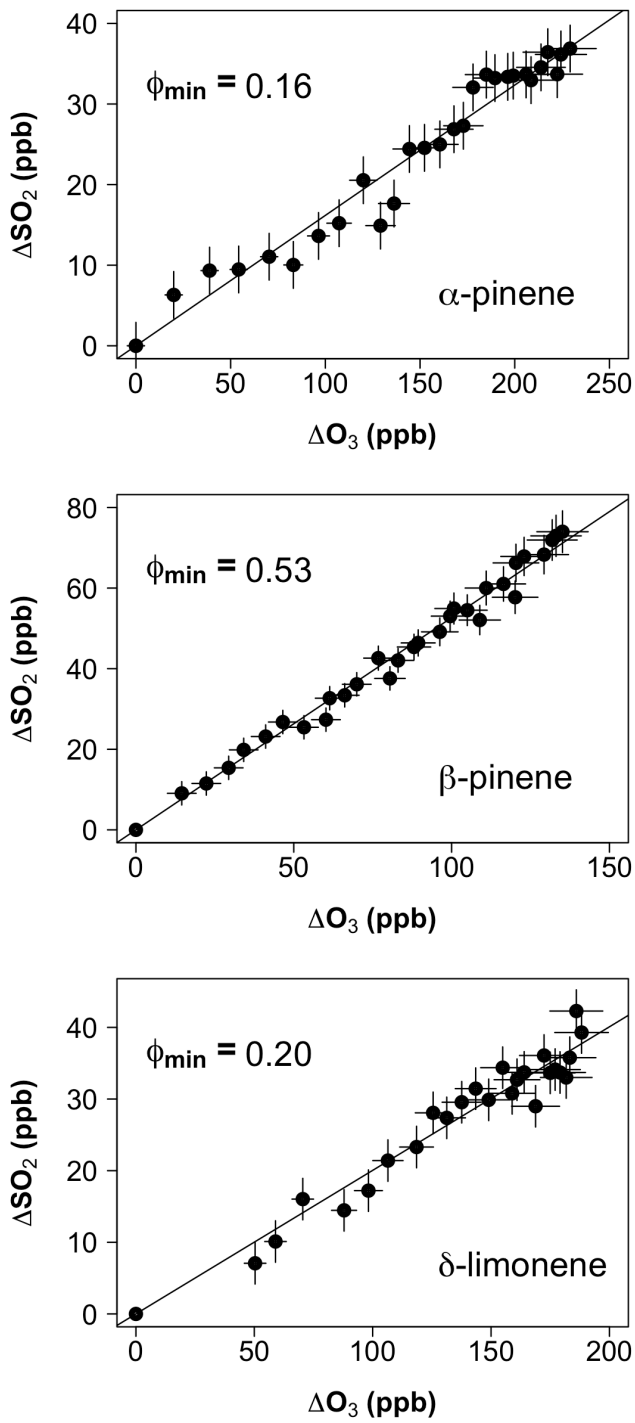

Figure 1. ΔSO_2 vs. ΔO_3 during excess SO_2 experiments ($[H_2O] < 5 \times 10^{15}$ cm^{-3}). The gradient determines the minimum SCI yield (ϕ_{min}).

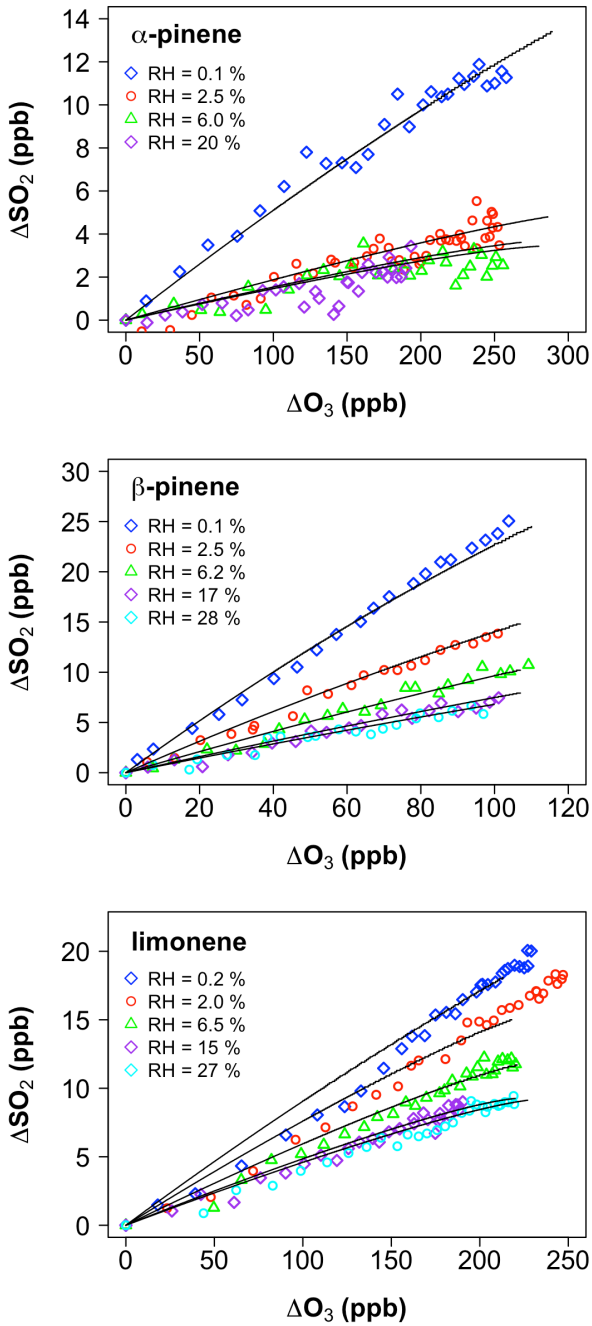

Figure 2. Cumulative consumption of SO_2 as a function of cumulative consumption of O_3, ΔSO_2 versus ΔO_3, for the ozonolysis of α-pinene, β-pinene and limonene in the presence of SO_2 at a range of water vapour concentrations, from 1×10^{15} cm^{-3} to 1.9×10^{17} cm^{-3}. Symbols are experimental data, corrected for chamber dilution. Lines are smoothed fits to the experimental data.

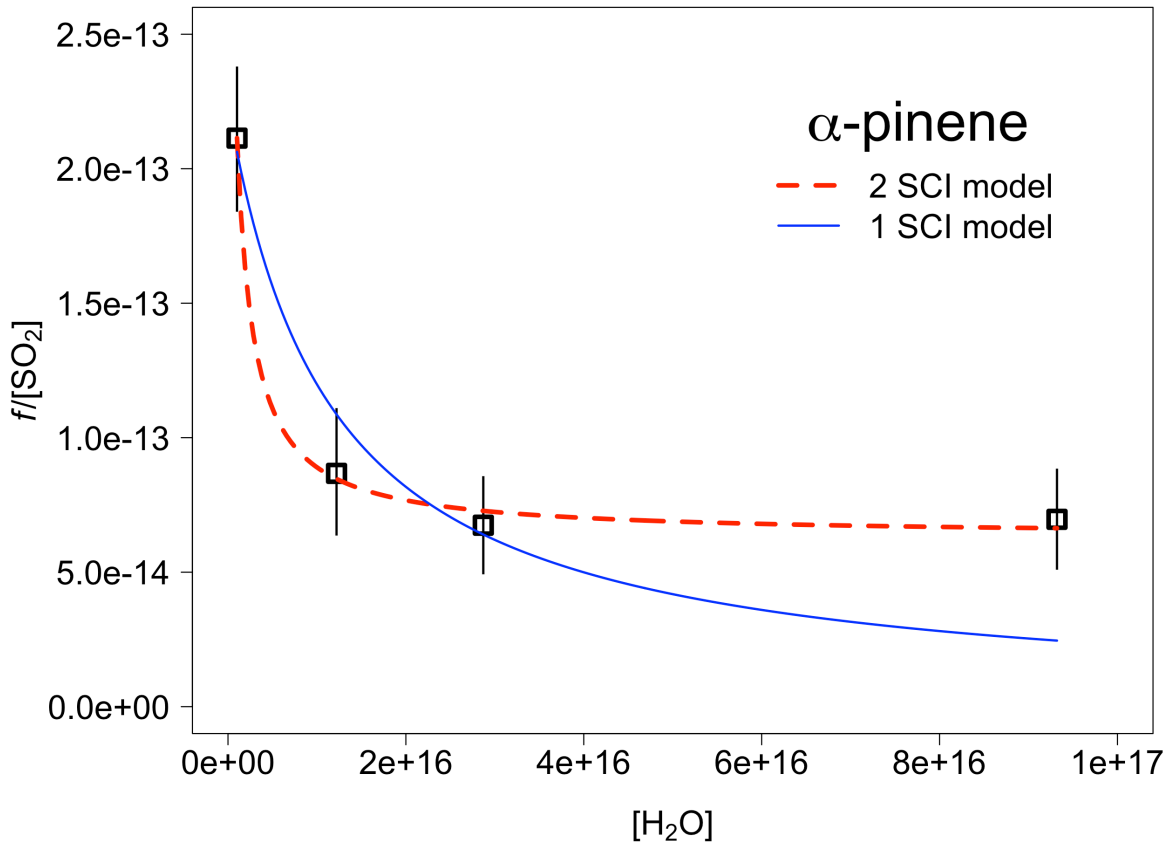

Figure 3. Application of a 2 SCI model fit (Equation E4) and a single SCI model fit (Equation E1) to the measured values (open squares) of $f/[SO_2]$ for α-pinene. From the fit we derive relative rate constants for reaction of the α-pinene derived SCI, SCI-A and SCI-B with H_2O (k_3/k_2) and decomposition ($(k_d+L)/k_2$) assuming that $\gamma^A = 0.40$ and $\gamma^B = 0.60$.

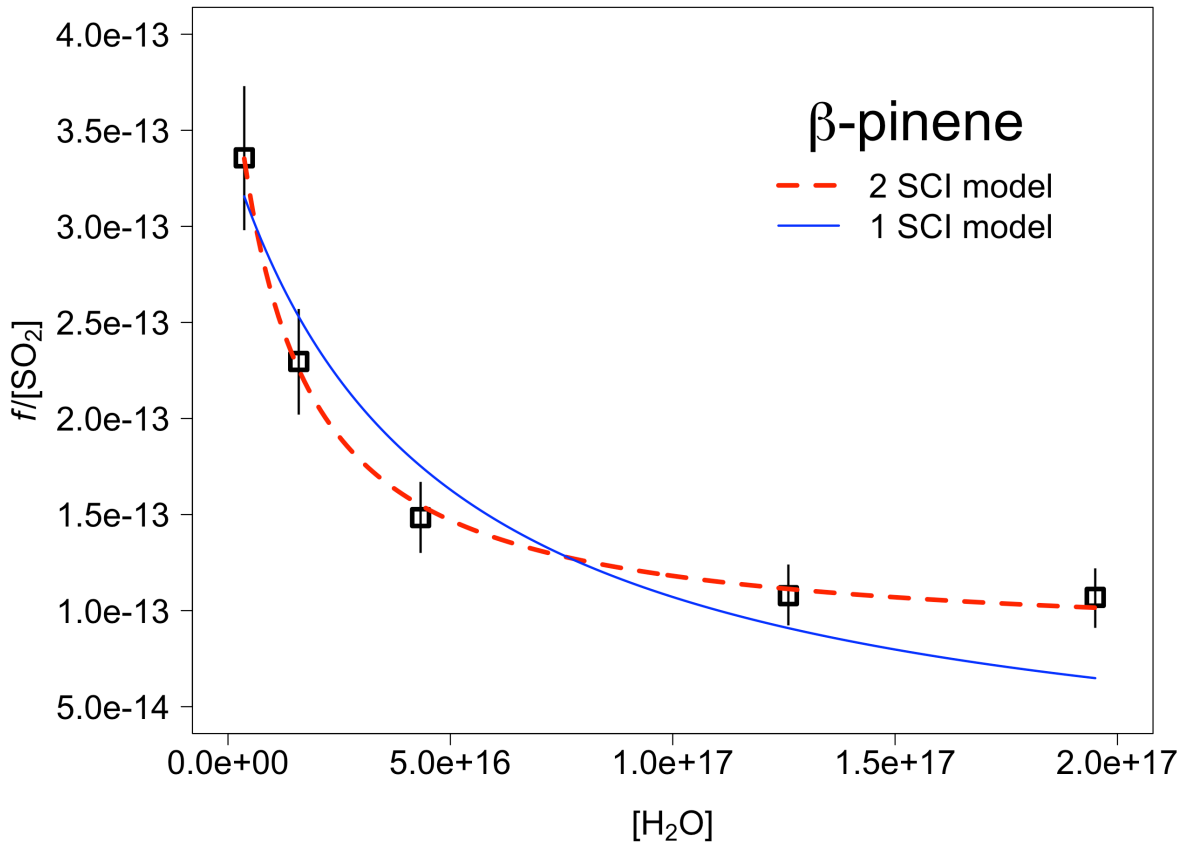

Figure 4. Application of a 2 SCI model fit (Equation E4) and a single SCI model fit (Equation E1) to the measured values (open squares) of $f/[SO_2]$ for β-pinene. From the fit we derive relative rate constants for reaction of the β-pinene derived SCI, SCI-A and SCI-B with H_2O (k_3/k_2) and decomposition ($(k_d+L)/k_2$) assuming that $\gamma^A = 0.41$ and $\gamma^B = 0.59$.

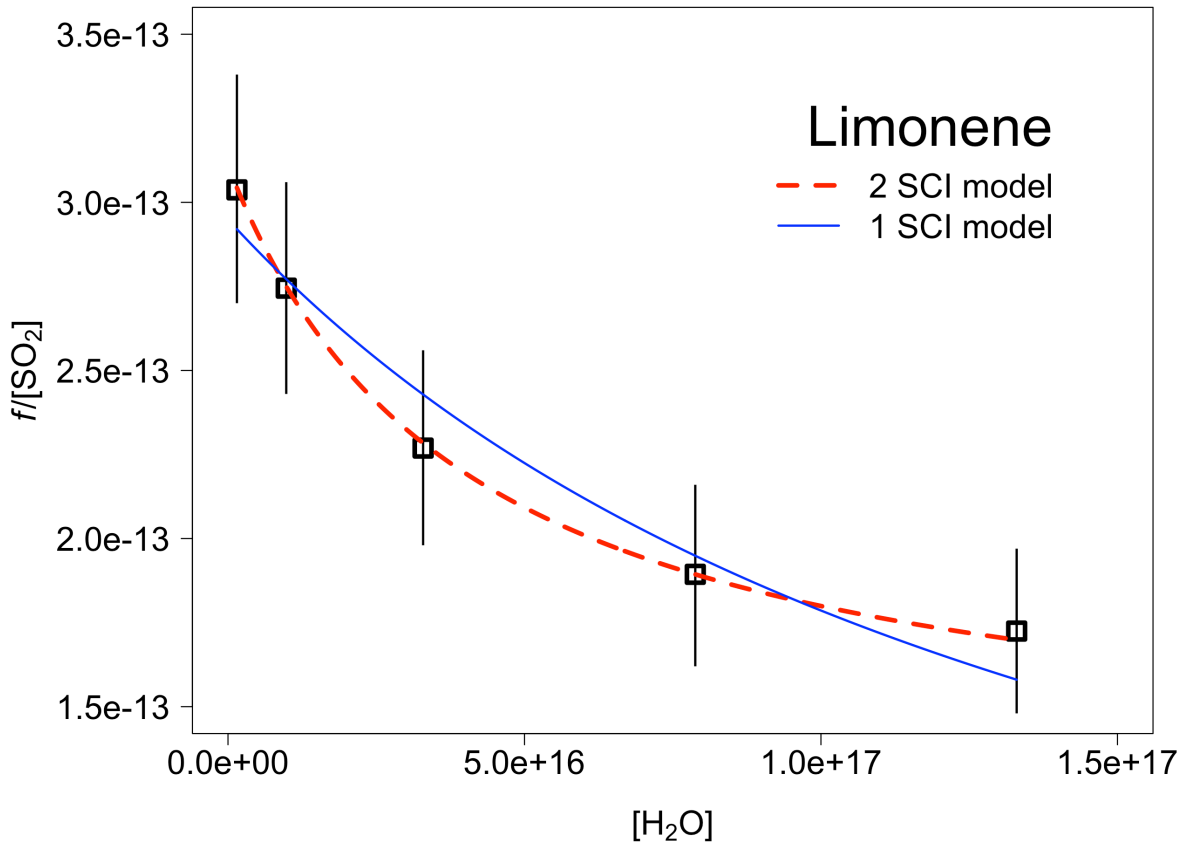

Figure 5. Application of a 2 SCI model fit (Equation E4) and a single SCI model fit (Equation E1) to the measured values (open squares) of $f/[SO_2]$ for limonene. From the fit we derive relative rate constants for reaction of the limonene derived SCI, SCI-A and SCI-B with H_2O (k_3/k_2) and decomposition ($(k_d+L)/k_2$) assuming that $\gamma^A = 0.22$ and $\gamma^B = 0.78$.

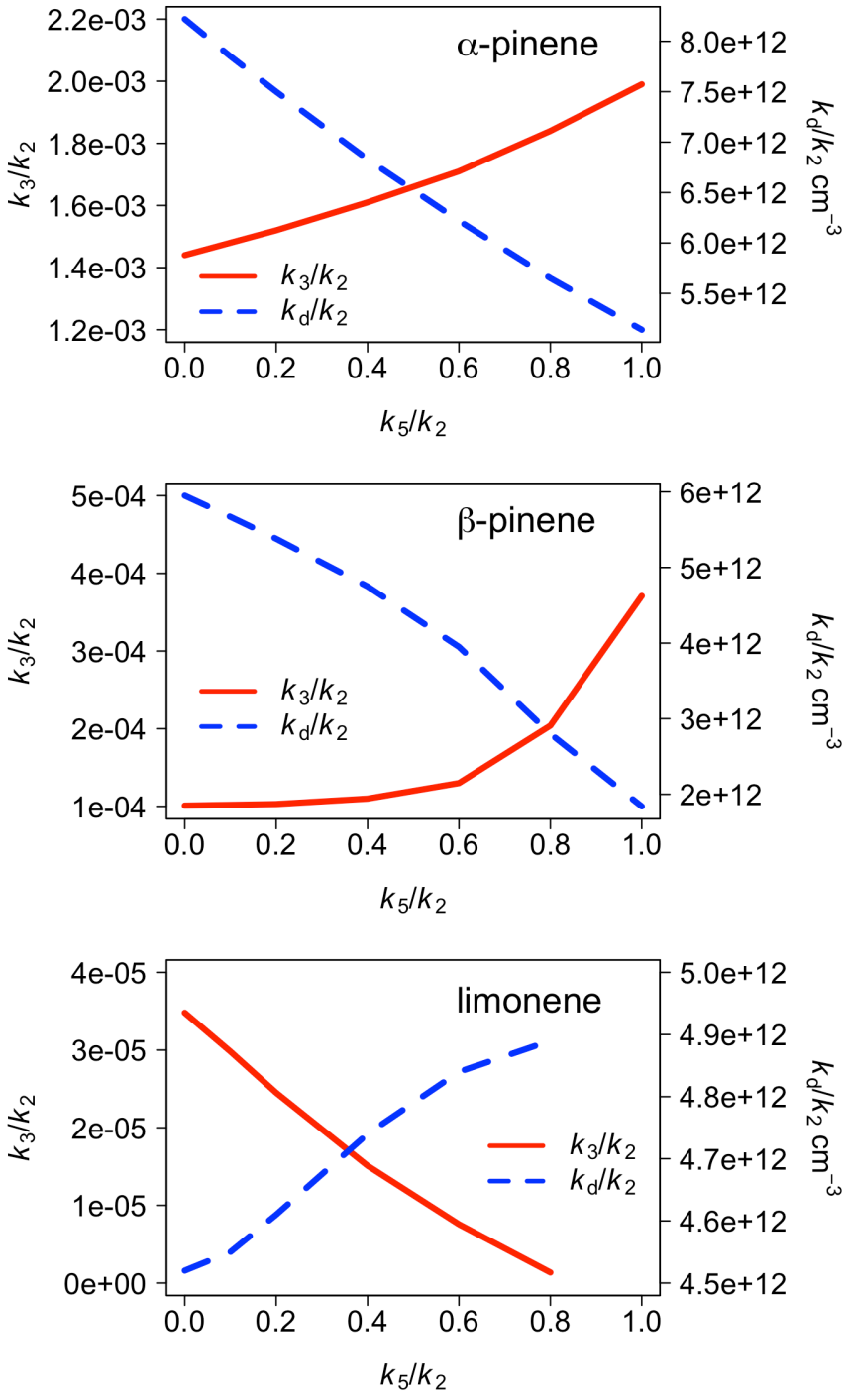

Figure 6. Variation of k_3/k_2 (k(SCI-A+H_2O))/(k(SCI-A+SO_2)) and k_d (k(SCI-B unimol.))/(k(SCI-B+SO_2)) as a function of the ratio k_5/k_2 (k(SCI+acid)/k(SCI+SO_2)), derived from least squares fit of Equation E4 to measurements shown in Figures 3 -5 for α-pinene, β-pinene and limonene respectively.

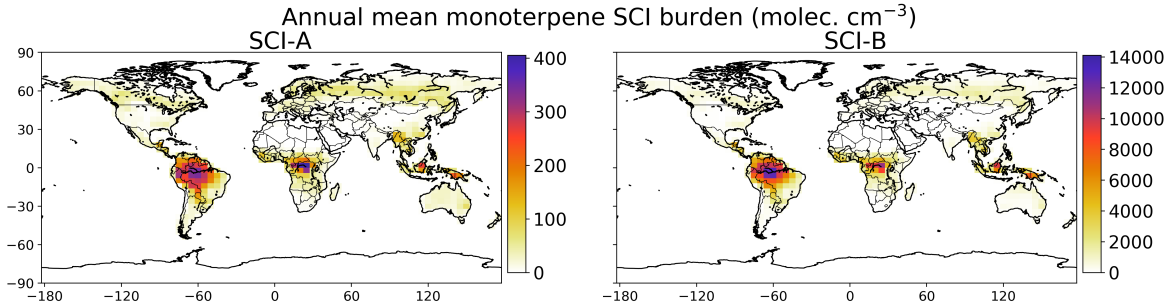

Figure 7. Annual mean monoterpene SCI-A and SCI-B concentrations (cm^{-3}) in the surface layer of the GEOS-Chem simulation.

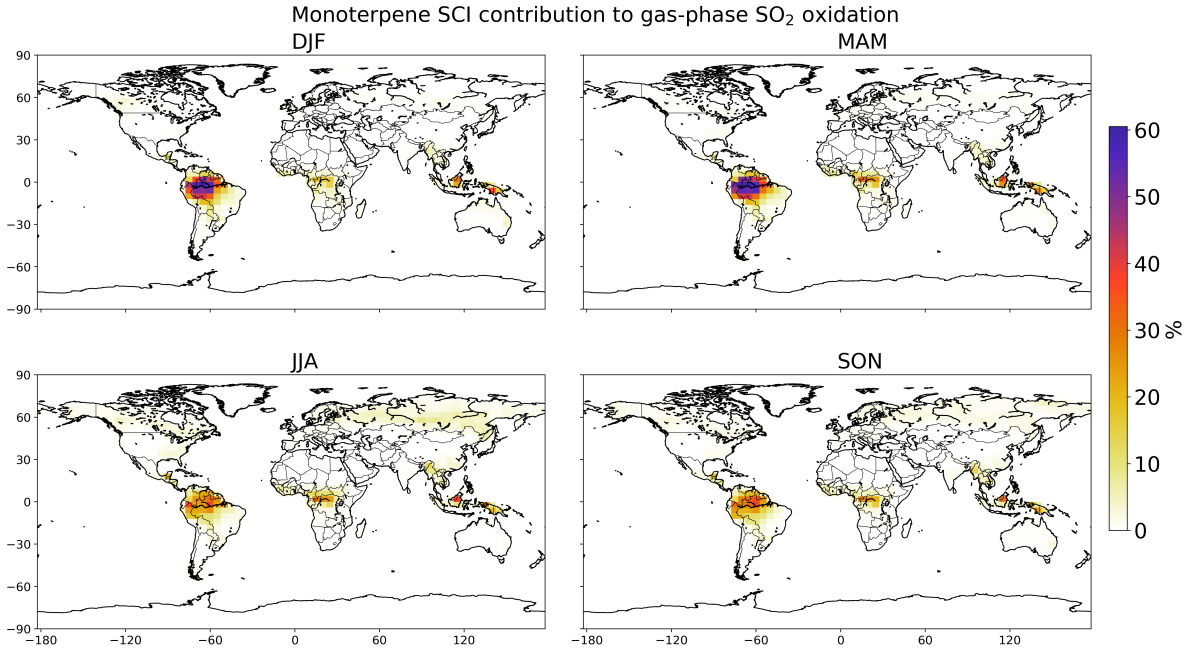

Figure 8. Seasonal SO_2 oxidation by monoterpene SCI as percentage of total gas-phase SO_2 oxidation in the surface layer.